

6. Abandonment of the South Penninic-Austroalpine paleosubduction plate interface zone, Central Alps: constraints from Rb/Sr geochronology

Abstract

The suture zone between lower-plate South Penninic and upper-plate Austroalpine units is crucial for understanding the early stages of plate convergence in the Central European Alps. Rb/Sr deformation ages for mylonitized rocks of the South Penninic paleosubduction *mélange* and for deformed Austroalpine basement shed light on the pre-Alpine and Alpine deformation history along the suture, as well as on the mode of syn-subduction interplate mass transfer. Rb/Sr age data define two age groups. The first group reflects the pre-Alpine, Paleozoic to Jurassic deformation within the upper plate basement, with varying degree of resetting by subsequent Alpine deformation. The second group marks the termination of subduction-related deformation along the South Penninic-Austroalpine suture zone at ~50 Ma. A foliation-parallel prograde mobilisate, precipitated at ~50 Ma within the subduction *mélange*, testifies to the presence of free fluids in the subduction channel. Identical Rb/Sr ages for pervasively deformed Austroalpine and South Penninic lithologies point to tectonic erosion of the upper plate during subduction. Elevated Sr isotope signatures of (meta-) carbonates from the South Penninic *mélange* are due to interaction of syn-subduction fluids with old continental crust. Lack of a metamorphic contrast between the South Penninic *mélange* and the Austroalpine upper plate favors exhumation of the suture zone due to a combination of tectonic underplating and erosion. Most likely, this underplating occurred when the Middle Penninic micro-continent entered the subduction zone. We propose that this process, at ~50 Ma, led to the cessation of deformation within the South Penninic *mélange*, shifted the zone of active deformation into the footwall, and also caused a contemporaneous upper plate uplift and shutoff of sedimentation in Alpine Gosau forearc basins.

6.1. Introduction

One key to understand the temporal evolution of fossil orogenic systems as analogues to recently active counterparts is isotopic dating of deformation processes. In this study we provide time constraints, based on Rb/Sr multimineral data, for the end of subduction-related deformation along the suture zone between the basal parts of the upper plate Austroalpine nappe stack and the South Penninic subduction *mélange* in the European Central Alps. Due to the scarcity of suitable mineral assemblages, related to the only low-grade metamorphism during Alpine deformation in the working area (diagenetic grade for

northernmost outcrops, higher greenschist grade for southernmost outcrops), a detailed study of the precise timing of Alpine deformation across and along this paleosubduction plate interface was still lacking. Hence, we investigated outcrops located in the eastern part of Switzerland (Fig. 6.1) along the fossil suture zone, representing samples from both the basal parts of the Austroalpine nappe stack and from the South Penninic *mélange* to clarify the timing of subduction-related deformation. For that purpose we made use of the Rb/Sr system of white mica and coexisting phases (feldspar, apatite, calcite, epidote) in intensely deformed rocks from both tectonic units. In our samples,

deformation and related white mica recrystallization occurred at temperatures well below 500°C - 550°C, ensuring preservation of Rb/Sr signatures related to dynamic recrystallization without major postdeformative diffusional resetting. Additionally, we studied the Rb/Sr isotope signature of 8 marine (meta-) carbonatic samples from the fossil plate interface zone for comparison with the Sr seawater evolution curve to get information about their age relationships and possible interaction with either crustal- or mantle-derived fluids.

The here studied plate interface zone resulted from subduction of the Penninic oceanic domain beneath the continental realm of the Adriatic plate (Austroalpine nappes) in Late Cretaceous - Early Tertiary (e.g. Froitzheim et al. 1996), prior to the onset of Alpine collision with the European margin. Froitzheim et al. (2003) suggested that the subduction zone of the South Penninic ocean was locked at ~50 Ma by the collision of the Middle Penninic micro-continent with the Adriatic margin, leading to the end of deformation along this suture zone at that time. Unfortunately, the authors provide no geochronological data for their time constraints. Large-scale differential tilting during exhumation of the fossil plate interface enables us to study this zone in present day outcrops, and provides access to various paleodepths (Figs. 6.1, 6.2). The exposed fossil plate interface has experienced flow and fracturing over an extended period of time, including minor overprint during Alpine continent-continent collision and subsequent exhumation. Nevertheless, it is shown that the fossil plate interface zone preserved its structural and isotopic record from the time when subduction-related deformation was terminated.

6.2. Geological framework

6.2.1. Alpine evolution

The European Alps, one of the best-studied mountain belts worldwide, resulted, in their present form, from the collision of the European and the Adriatic continental plates (Austroalpine nappe stack), preceded by southeastward to southward subduction and accretion of the intervening Penninic oceanic domain (Fig. 6.1). Most models differentiate between two 'Alpine' orogenic cycles: A Cretaceous orogenic cycle (referred to as 'Eoalpine', e.g. Wagnreich 1995) is characterized by an east to southeast dipping subduction zone resulting in the closure of the Meliata ocean and leaving signatures of subduction-related deformation within the Austroalpine nappes (belonging to the Adriatic plate, e.g. Schmid et al. 2004). Stacking within the Austroalpine units is associated with top-W, locally top-SW and top-NW thrusting (Froitzheim et al. 1994, Handy 1996). The direction of convergence changed to north - south during the Tertiary orogenic cycle (referred to as 'Mesoalpine' to 'Neoalpine', e.g. Wagnreich 1995) with top-N thrusting and closure of the Alpine Tethys in between the European and Adriatic plates (Froitzheim et al. 1994, Handy 1996, Schmid et al. 2004). According to Froitzheim et al. (1994) the transition between top-W thrusting and top-N thrusting is marked by a Late Cretaceous extensional phase with top-SE directed normal faulting, which partly reactivates deformation features of the former deformational stages. This clear separation between the Cretaceous and the Tertiary orogenic cycle is only well observable in the Austroalpine nappes of the Eastern Alps (e.g. Schmid et al. 2004). However, subduction and accretion of oceanic units in the Western Alps represents a continuous process from the Late Cretaceous to the Paleogene, transforming a passive continental margin into an active

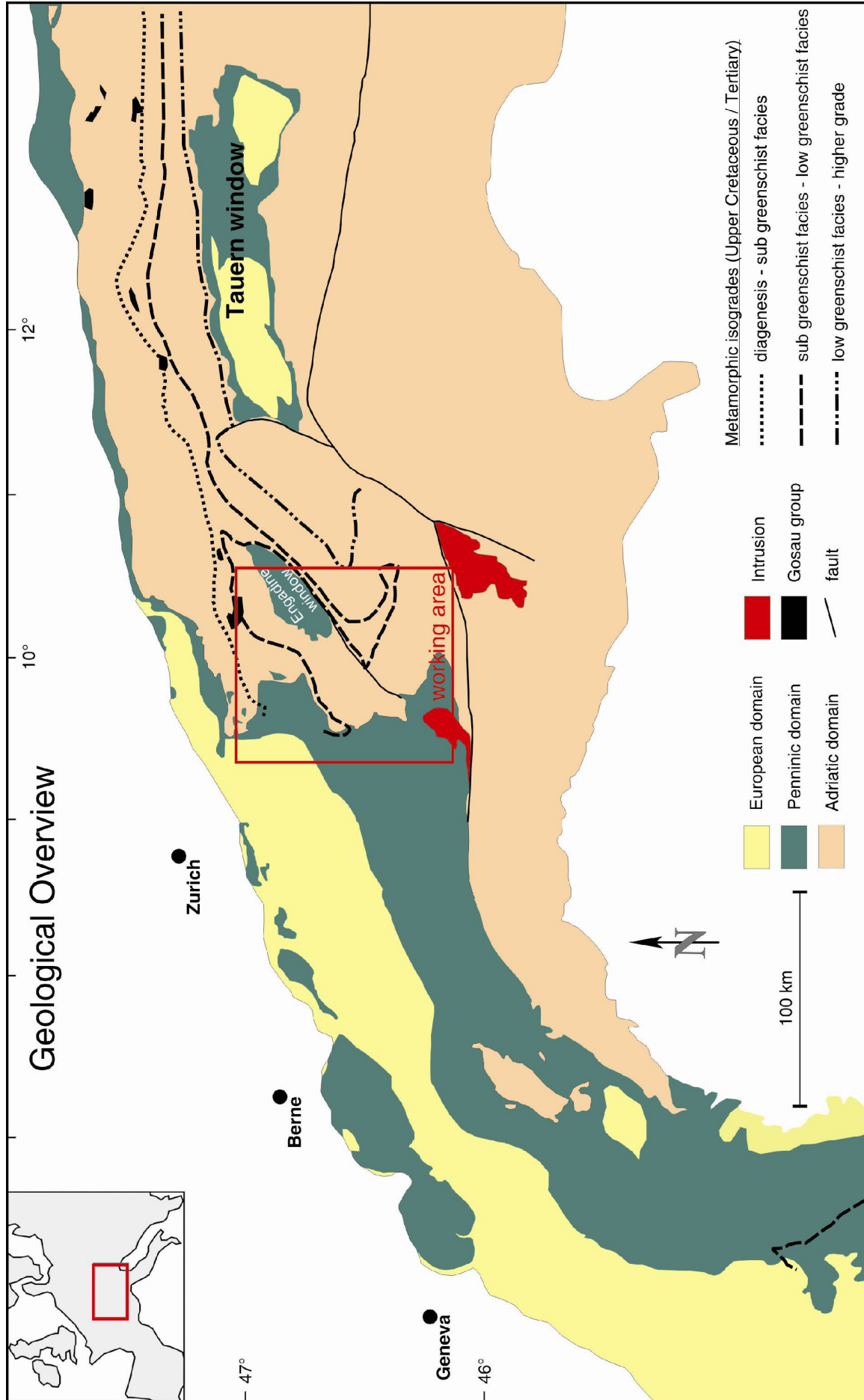


Figure 6.1: Simplified geological map of the European Alps, modified after Frey et al. (1974) and Stampfli et al. (2002). Metamorphic isogrades redrawn after Frey et al. (1999). Rectangle delineates the working area in the Central Alps. Note, the Adriatic domain comprises the Austroalpine nappe stack.



one (i.e. with an active subduction zone, e.g. Schmid et al. 2004).

The oceanic units in between both continental realms (European and Adriatic plate), the Penninic units (Fig. 6.1), were progressively subducted and deformed during convergent plate motion and partly accreted to the front and / or the base of the Adriatic plate. Palinspastic restoration of the Penninic units resulted in two separate oceanic basins divided by a micro-continent (e.g. Florineth & Froitzheim 1994, Schmid et al. 2004). This so-called Briançonnais terrane (or Middle Penninic) separates the northern basin (North Penninic or Valais ocean) from the southern basin (South Penninic or Piemont-Liguria ocean). Fragments from the Piemont-Liguria ocean experienced high pressure metamorphism in the Western Alps during the Tertiary, whereas South Penninic units in the Eastern Alps are characterized by a Cretaceous tectonic imprint associated with variable grades of metamorphism ranging from diagenesis to blueschist facies (Schmid et al. 2004). Owing to the fact that the paleosubduction interface has been tilted and differentially exhumed from original depth, we are able to study it in present day outcrops.

6.2.2. *Geology of the working area*

The working area is located in the Central Alps of Eastern Switzerland (Figs. 6.1, 6.2). The main geological units in the area belong to either the South Penninic or the Austroalpine units. In various plate tectonic models the Austroalpine domain

overrides the South Penninic domain during Cretaceous/ Tertiary subduction (e.g. Ring et al. 1988, Schmid et al. 2004). Therefore, the immediate plate interface zone between the South Penninic domain (Arosa zone and the Platta nappe as its direct equivalent to the south [Biehler 1990], Fig. 6.2) and the Austroalpine represents a Late Cretaceous/ Tertiary continent-ocean suture (e.g. Handy 1996, Schmid et al. 2004) of a convergent plate margin. The large-scale structures of the Arosa zone are interpreted by e.g. Ring et al. (1988, 1989, 1990) as the deep parts of an accretionary wedge formed at the tip of and below a thrust belt migrating towards the west. The apparent thickness of the South Penninic domain in the study area varies from a few tens of meters up to more than 2500 m, either reflecting the original thickness or a reduction by subsequent thinning processes.

Ring et al. (1990) pointed out that the lithofacies and the internal structures of the Arosa zone are comparable to characteristics of mélanges found within subduction complexes. Therefore, the South Penninic domain is discussed as a (subduction) mélange of both oceanic material (derived from the South Penninic ocean) and continental fragments (derived from the Austroalpine domain) (Deutsch 1983, Ring et al. 1988 and references therein). Within the subduction mélange, competent blocks of Austroalpine and South Penninic affinity are embedded in a less competent matrix composed of serpentinites or calcareous shales (Ring et al. 1990). Deformation is partitioned into brittle and ductile due to competence contrasts between clasts and matrix (Ring et al. 1988). Metamorphic conditions of South Penninic rocks range from upper diagenetic or lowermost greenschist facies in the north of the working area, to middle to upper greenschist facies in the southern parts (Figs. 6.1, 6.2). The Austroalpine domain consists of a suite of gneissic to amphibolitic, mainly upper crustal rocks

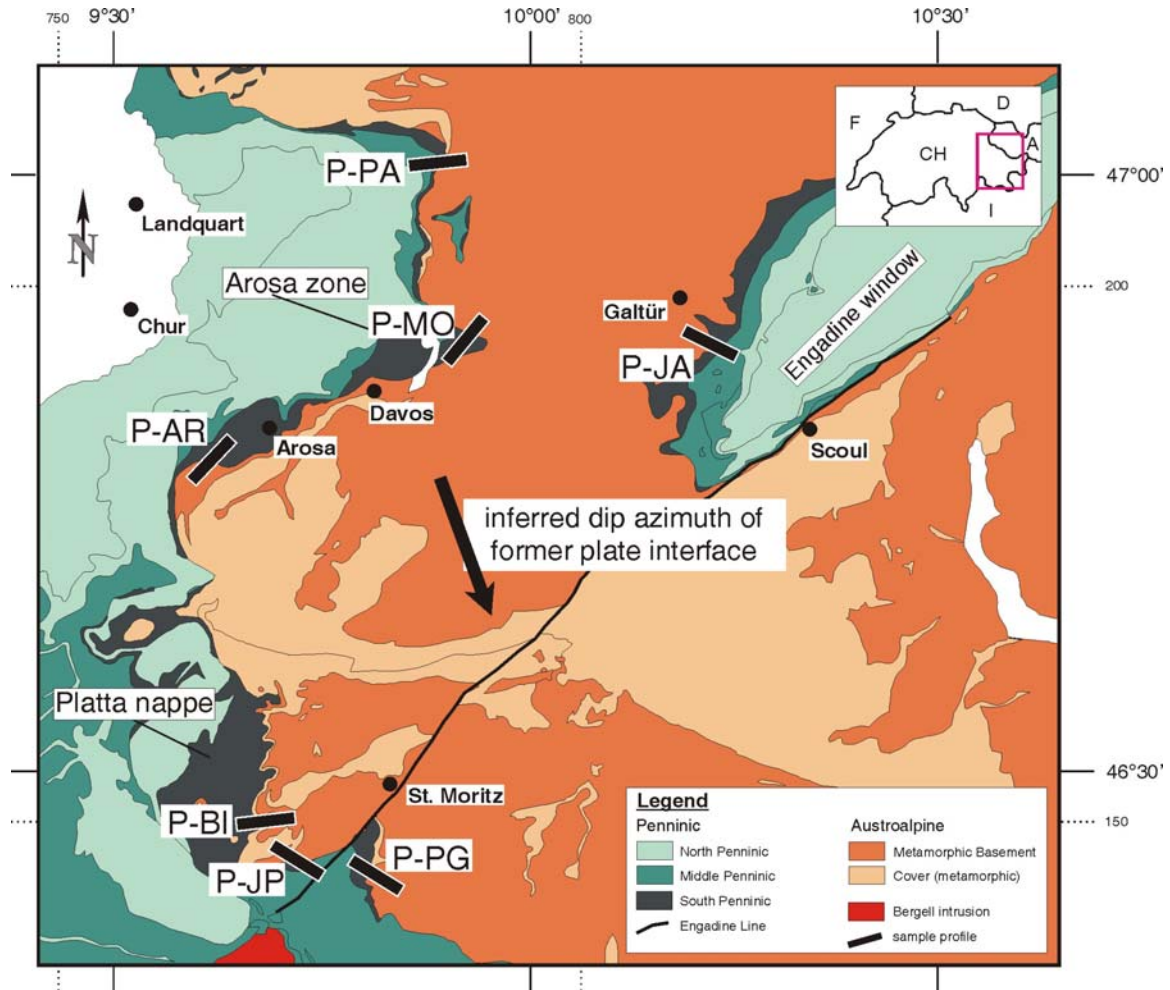


Figure 6.2: a) Tectonic map of the study area emphasizing the suture zone between the South Penninic (black) and the Austroalpine (dashed, part of the Adriatic plate). Black lines indicate different profiles extending from domains of South Penninic origin into Austroalpine rocks. Arrow points to the former dip azimuth of the plate interface. Arosa zone and Platta nappe are local names for rocks of South Penninic affinity. Based on the Tectonic map of Switzerland 1:500.000, 2nd edition (1980).

which experienced pre-Alpine (mainly Permo-Carboniferous) and Early (Eo-) Alpine deformation, overlain by and intercalated with variably deformed and metamorphosed Permo-Carboniferous clastic rocks, and Mesozoic sediments (e.g. Florineth & Froitzheim 1994, Manatschal et al. 2003, Ring et al. 1988). Due to large scale differential post-subduction tilting and exhumation of the fossil plate interface zone formerly deeper parts are accessible towards the south.

In analogy to active convergent plate margins we consider the South Penninic subduction mélangé to resemble material of a so-called subduction channel (e.g.

Cloos and Shreve, 1988 a, b; Chapter 4). Cloos and Shreve (1988 a, b) have introduced the subduction channel concept denoting a zone between the upper and the lower plates of convergent plate margins. This zone may typically be up to a few kilometers wide, its material exhibiting a velocity gradient towards both plates, and it probably extends to a depth of more than 100 km (Gerya and Stöckhert 2002). Within the subduction channel, material from both the oceanic and continental plates is intermingled and transported downwards. The channel material may then either get lost into the earth's mantle, it may be partly off-scraped and accreted to the front of a growing accretionary wedge

(frontal accretion), or accreted to the base of the hanging wall (basal accretion) (von Huene and Scholl 1991). Material may also be removed from the tip (frontal tectonic erosion) or the base (basal tectonic erosion) of the upper plate by tectonic erosion (e.g. Clift and Vannucchi 2004). Clasts within the matrix of the subduction mélange provide hints for dominance of tectonic erosion or accretion. According to Oncken (1998) abundance of upper plate fragments in the channel material is a diagnostic criterion for the role of tectonic erosion. Basal tectonic erosion as prevailing mass transfer mode along the South Penninic-Austroalpine plate interface zone is indicated by numerous clasts of upper plate material embedded within the South Penninic mélange (Chapter 4).

6.2.3. Structural aspects of the fossil plate interface zone

We measured foliation, lineation, shear bands, tension gashes, folds, faults, and assessed their relative age relationships in a series of profiles across the plate interface, sampling different paleodepths of the paleosubduction zone (Fig. 6.3). The South Penninic mélange close to the contact to the Austroalpine upper plate experienced a penetrative deformation with an inferred direction of tectonic transport changing gradually from top-NW in the north of the working area via top-W in the central parts to top-SW in the southernmost parts (e.g. Chapter 4). This might be explained by oblique subduction, which favors partitioning of deformation. We observed foliation planes dipping moderately toward SE to NE and associated stretching lineations plunging smoothly toward SE and ENE (Fig. 6.3, see also Fig. 4.5 in Chapter 4). These structures are best developed in the south of the working area. Embedded clasts within the matrix of the South Penninic mélange are partly bounded by shear zones

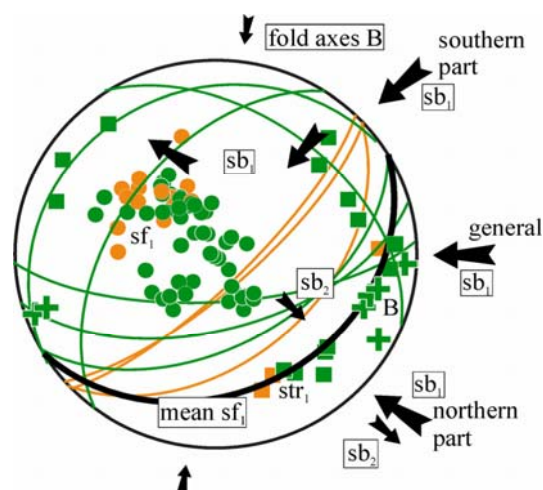


Figure 6.3: Combination of structural data of brittle-ductile to ductile deformation associated with top-NW (northern part of the working area) to top-SW (southern part of the working area) direction of tectonic transport (general top-W, large black arrows). Data are subdivided in: green corresponding to outcrops located within the South Penninic mélange, orange corresponding to outcrops located within the basal parts of the Austroalpine upper plate. Plot is a Schmidt net lower hemisphere, equal-area diagram. In addition, subsequent non-pervasive deformation is indicated (top-SE extension and top-N thrusting, small black arrow). Note that there is no obvious difference in the structural data obtained from outcrops in the South Penninic mélange and the Austroalpine upper plate. See text for data. str = stretching lineation, sf = foliation, B = fold axes, sb = shear bands

also pointing to a general top-W direction of tectonic transport. Deformation of the South Penninic mélange increases towards the south of the working area, which is expressed by a more distinct and tighter foliation, and by the obliteration of sedimentary structures. Deformation with general top-W directed tectonic transport of the Austroalpine nappe stack is expressed by microscale fracture zones reactivating the preexisting foliation of probably Variscan age in the northern part of the working area (Chapter 4). This overprint increases towards the south, where Alpine deformation pervasively overprints the preexisting foliation within at least the basal parts of the upper plate basement. This is expressed by growth and recrystallization of platy minerals (mainly

white mica) parallel to the preexisting foliation. Orientation of foliation in the Austroalpine rocks parallels the corresponding foliation within the South Penninic mélange, at least in the first few hundred meters above the base of the hanging wall. In general, orientation of structural data and the therewith assessed direction of tectonic transport are similar in both the South Penninic mélange and the basal parts of the Austroalpine upper plate (Fig. 6.3).

Subsequent localized deformation with significantly lower intensity overprints the top-W structures, but a complete erasure of the top-W structures in both the South Penninic mélange and the Austroalpine nappes by younger deformational processes cannot be observed (see also Ring 1989, Dürr 1992). There is a superimposed set of brittle-ductile shear bands indicating top-E to top-SE directed tectonic transport, a feature becoming more prominent towards the south (Fig. 6.3). All the above structures are overprinted by top-N thrusting. This shortening direction can be inferred from roughly E-W orientated fold axes of open folds at various scales (Fig. 6.3, Chapter 4).

6.3. Published age data

Time constraints on the evolution of the South Penninic mélange are sparse; the few existing data are summarized below (Fig. 6.4). Ocean spreading, and thus opening of the South Penninic ocean, is dated to have occurred at least since the Early to Middle Jurassic (186 ± 2 Ma Ar/Ar bt, Ratschbacher et al. 2004, 165 Ma Ar/Ar phl, Gebauer 1999). According to Wagreich (2001) and references therein, the transition to an overall convergent setting and the initiation of oblique southward subduction of the Penninic domain beneath the Austroalpine occurred during the Aptian/ Albian, at ~ 110 Ma.

Biostratigraphic ages provide additional constraints on the timing of subduction-related deformation of the South Penninic mélange. Latest sedimentation within the Arosa zone (South Penninic) is documented to have occurred within the Early Coniacian, at ~ 90 Ma (Late Cretaceous, Ring 1989). Flysch deposits from the Platta nappe (South Penninic) show sedimentation ages ranging from Aptian to Albian (late Early Cretaceous; Ring 1989). Overall, no sediments younger than ~ 90 Ma are known from the South Penninic mélange. Biostratigraphic ages for the flysch deposits comprising the footwall of the South Penninic mélange (derived from Middle and North Penninic units, and from the distal European margin, Figs. 6.2, 6.4) range from Early Cretaceous to Early/ Middle Eocene (Trautwein et al. 2001). In addition, Stampfli et al. (2002) reported distal flysch deposition until 43 Ma. In consequence, subduction-related sedimentation lasted at least until the Late Cretaceous to the Early/ Middle Eocene, a time span between ~ 90 Ma to 43 Ma (passage through the subduction channel from termination of sedimentation within the South Penninic ocean to latest sedimentation within the flysch accreted at the base of the South Penninic domain).

Constraints on the timing of subduction-related deformation are also given by isotopic ages pointing to 90 Ma - 60 Ma for a pressure-dominated metamorphism of the Lower Austroalpine units, and 60 Ma to 35 Ma for the South Penninic and European units, respectively (Handy and Oberhänsli 2004, and references therein). Schmid et al. (2004) reported HP metamorphism of South Penninic rocks during the Tertiary, at least for the Western Alps. Handy and Oberhänsli (2004, and references therein) reported thrusting and accreting under HP-greenschist facies conditions during a time span between 88 Ma and 76 Ma for the Austroalpine domain in the southern part of our study area. Earliest high-pressure metamorphism for

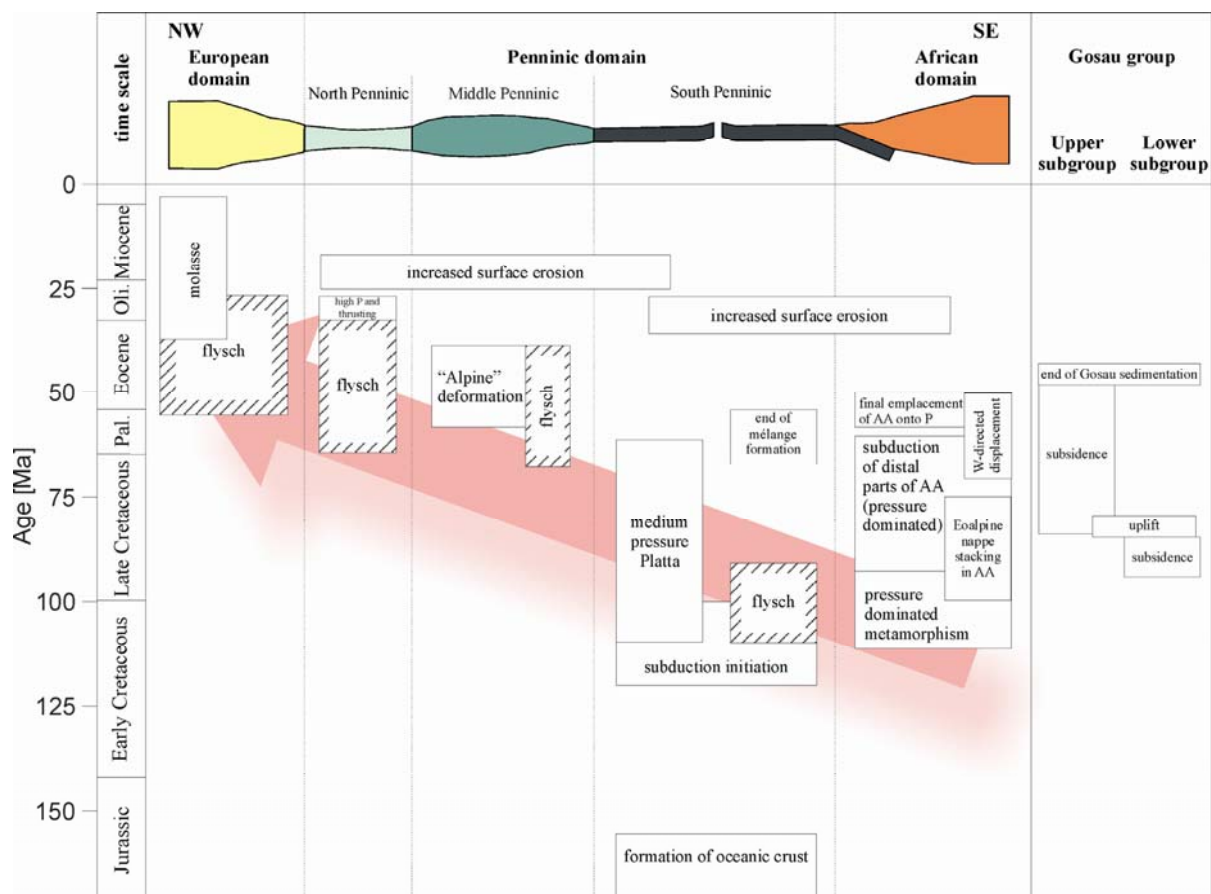


Figure 6.4: Compilation of geochronological data available for the study area concerning the subduction and accretion of the South Penninic domain, deformation within the Austroalpine nappe stack, flysch deposition within the South Penninic domain and its footwall, and deformation within the Middle Penninic, North Penninic and European units. Subsidence and sedimentation history of the Gosau group is also indicated. Light red arrow indicates shift in subduction-related deformation towards the foreland (i.e. towards NW). See text for details and source of data.

parts of the Penninic domain further to the east (Tauern Window) is constrained to 57 ± 3 Ma for the subduction-accretion Rechnitz complex (Ar/Ar amphibole, Ratschbacher et al. 2004). Additionally, Markley et al. (1995) used Ar/Ar geochronology on synkinematic white mica from Middle Penninic (Briançonnais domain) rocks. They obtained ages at around 38 Ma. Together, these data show the migration of subduction and therewith related deformation towards the foreland (i.e. towards NW in modern coordinates), which finally culminated in the collision with the European margin (Fig. 6.4). The northwestward younging of flysch deposition ages is consistent with this

migration (e.g. Handy and Oberhänsli 2004, and references therein).

Constraints for the timing of unstable slip within the basal parts of the Austroalpine upper plate are given by Thöni (1981, 1988). The author presented K/Ar and Rb/Sr data from pseudotachylytes collected along the northwestern part of the Engadine window. Presence of pseudotachylytes is considered as evidence for paleoearthquakes (Cowan 1999). These pseudotachylytes yielded ages of approximately 75 Ma. Additionally, we obtained $^{40}\text{Ar}/^{39}\text{Ar}$ ages using stepwise heating with a laser system, in order to better constrain the generation of pseudotachylytes within the basal parts of

the Austroalpine nappe stack at the northwestern rim of the Engadine window. This resulted in an expanded time window for the occurrence of unstable slip between 60 Ma and 80 Ma (see Chapter 5).

6.4. Analytical procedures for Rb/Sr geochronology and Sr isotope signature

For the purpose of Rb/Sr isotope analyses we used the internal mineral isochron approach (Glodny et al. 2002, 2005). Samples of small size (approximately 20 - 100 g) were chosen, carefully selected as, wherever viable, texturally exclusively recording a specific recrystallization-inducing tectonic and metamorphic event. In our study this is the pervasive general top-W directed tectonic transport within the South Penninic mélangé and basal parts of the Austroalpine domain, related to the subduction of Penninic units underneath the Austroalpine nappe stack. We focused on samples containing white mica as a high Rb/Sr phase. The Rb/Sr isotope system of white mica is assumed to be thermally stable to temperatures $>500^{\circ}\text{C} - 550^{\circ}\text{C}$, but may be fully reset by dynamic recrystallization even at lower temperature (Inger and Cliff 1994, Freeman et al. 1997, Villa 1998). According to Müller et al. (1999) isotopic reequilibration between white mica and coexisting phases during mylonitization may occur at temperatures as low as 350°C . Careful study of the correlation between microtextures and isotopic signatures, both by conventional mineral separation techniques (Müller et al. 1999, Glodny et al. submitted) and Rb/Sr microsampling (Müller et al. 2000, Cliff and Meffan-Main 2003) has shown that complete synkinematic recrystallization in mylonites is usually accompanied by isotopic reequilibration. Therefore, Rb/Sr isotopic data from penetratively deformed rocks can be used to date the waning stages of mylonitic deformation, as long as deformation occurred below the temperature range for

diffusional resetting. In our samples, deformation and related white mica recrystallization occurred at temperatures well below 500°C to 550°C (calcmylonites, subgrain rotation recrystallization in quartz, brittle deformation of feldspar, Chapter 4), which makes sure that Rb/Sr isotopic signatures record dynamic recrystallization under greenschist facies conditions without subsequent diffusional resetting. To detect possible Sr isotope inhomogeneities resulting from isotopic inheritance, from long-term or incomplete dynamic recrystallization, from diffusional Sr redistribution, and/or from alteration processes, white mica was analysed in several, physically different (in terms of magnetic properties and/or grain size) fractions whenever possible. According to Müller et al. (1999) this approach ensures control on possible presence of unequilibrated, pre-deformational white mica relics. In addition, mineral concentrates of feldspar, apatite, calcite, and epidote were produced. Care was taken to exclude material altered by weathering or by late fluid-rock interaction. White mica sieve and magnetic fractions were ground in ethanol in an agate mortar, and then sieved in ethanol to obtain pure, inclusion-free separates. All mineral concentrates were checked, and finally purified by hand-picking under a binocular microscope. Rb and Sr concentrations were determined by isotope dilution using mixed $^{87}\text{Rb} - ^{84}\text{Sr}$ spikes. Determinations of Rb and Sr isotope ratios were carried out by thermal ionization mass spectrometry (TIMS) on a VG Sector 54 multicollector instrument (GeoForschungsZentrum Potsdam). Sr was analyzed in dynamic mode. The value obtained for $^{87}\text{Sr}/^{86}\text{Sr}$ of NBS standard SRM 987 was 0.710268 ± 0.000015 ($n = 19$). The observed Rb isotopic ratios were corrected for 0.25% per a.m.u. mass fractionation. Total procedural blanks were consistently below 0.15 ng for both Rb and Sr. Because of generally low and highly variable blank

values, no blank correction was applied. Isochron parameters were calculated using the Isoplot/Ex program of Ludwig (1999). Standard errors, as derived from replicate analyses of spiked white mica samples, of $\pm 0.005\%$ for $^{87}\text{Sr}/^{86}\text{Sr}$ ratios, and of $\pm 1.5\%$ for Rb/Sr ratios were applied in isochron age calculations (cf. Kullerud 1991). Individual analytical errors were generally smaller than these values. Rb/Sr analytical data are given in Table 1.

Additionally, we studied the Rb/Sr isotope signatures of 8 originally marine (meta-) carbonatic samples from the fossil plate interface zone. The Sr-isotopic ratio of seawater is known to vary with time (e.g. Wickman 1948, Gast 1955), so that Sr isotopic compositions of seawater precipitates (e.g. biogene carbonates) may directly be converted to absolute age information ('strontium isotope stratigraphy', Howarth and McArthur 1997, McArthur et al. 2001). In our analytical protocol we dissolved the carbonate samples with 2.5N HCl and monitored Rb contents and Rb/Sr ratios of the samples, to be able to correct for potential in-situ radiogenic ingrowth of Sr.

6.5. Petrography and sampling

The South Penninic subduction *mélange* exhibits a N-S gradient in metamorphic grade. In the northern part of the working area, Alpine metamorphism did not exceed diagenetic grades, or lower greenschist facies (see also Chapters 4, 6.2). In the southern part, rocks of the *mélange* as well as the basal parts of the Austroalpine nappe stack were metamorphosed at middle to upper greenschist-facies conditions during Alpine orogeny (as inferred from Si contents in phengitic white mica, e.g. Chapter 4). Along this N-S profile, we sampled calcsilicates, calcmylonites, quartz-mica schists and a quartz-mobilisate (mineralized vein) from the South Penninic *mélange*, as well as quartz mylonites,

mylonitized Permian meta-volcanics and quartz-mica schists from the basal parts of the Austroalpine nappe stack (Figs. 6.5a-i). Samples used for Rb/Sr dating are fine grained, strongly foliated or mylonitized, except for the qtz-mobilisate. Minerals found in these rocks include quartz, feldspar, white mica, biotite, calcite, apatite, opaque minerals, and epidote. Locally, retrograde chlorite occurs. The mineral assemblages in general testify to greenschist-facies conditions during deformation in both the basal parts of the upper plate and the subduction *mélange*. The strong deformation (Figs. 6.5e, f) caused, in most samples, optically complete to nearly complete recrystallization of white mica, apatite, calcite, and albite. Samples show a general top-W direction of tectonic transport (Fig. 6.3). However, overprint by subsequent deformation (top-SE, top-N) is visible to some extent in the field, which is expressed by e.g. a crenulated foliation. We omitted samples with stronger overprint by identifying overprinting relationships at outcrop scale or within thin sections in order to date only a single deformation event (top-W). In the following, the description of the different samples is organized from north to south, and separated between samples for Rb/Sr geochronology, and Sr isotope signature. Mineral abbreviations follow Kretz (1983). The locations of the geochronological samples are shown in Figure 6.6, locations of samples used for Sr isotope signature analyses are shown in Figure 6.7.

Sample 4d represents a mylonite from the base of the upper plate at the northernmost profile P-PA (Fig. 6.6). It consists of heavily sericitized fs (kfs 50 mole-%, ab 45 mole-%, an 5 mole-%), qtz showing subgrain rotation recrystallization, ms (Si p.f.u. 3.15 – 3.24), and minor ap. Foliation is expressed by the alignment of both white mica and feldspar-quartz rich layers. Larger feldspar grains form clasts, which are oriented subparallel to the foliation.

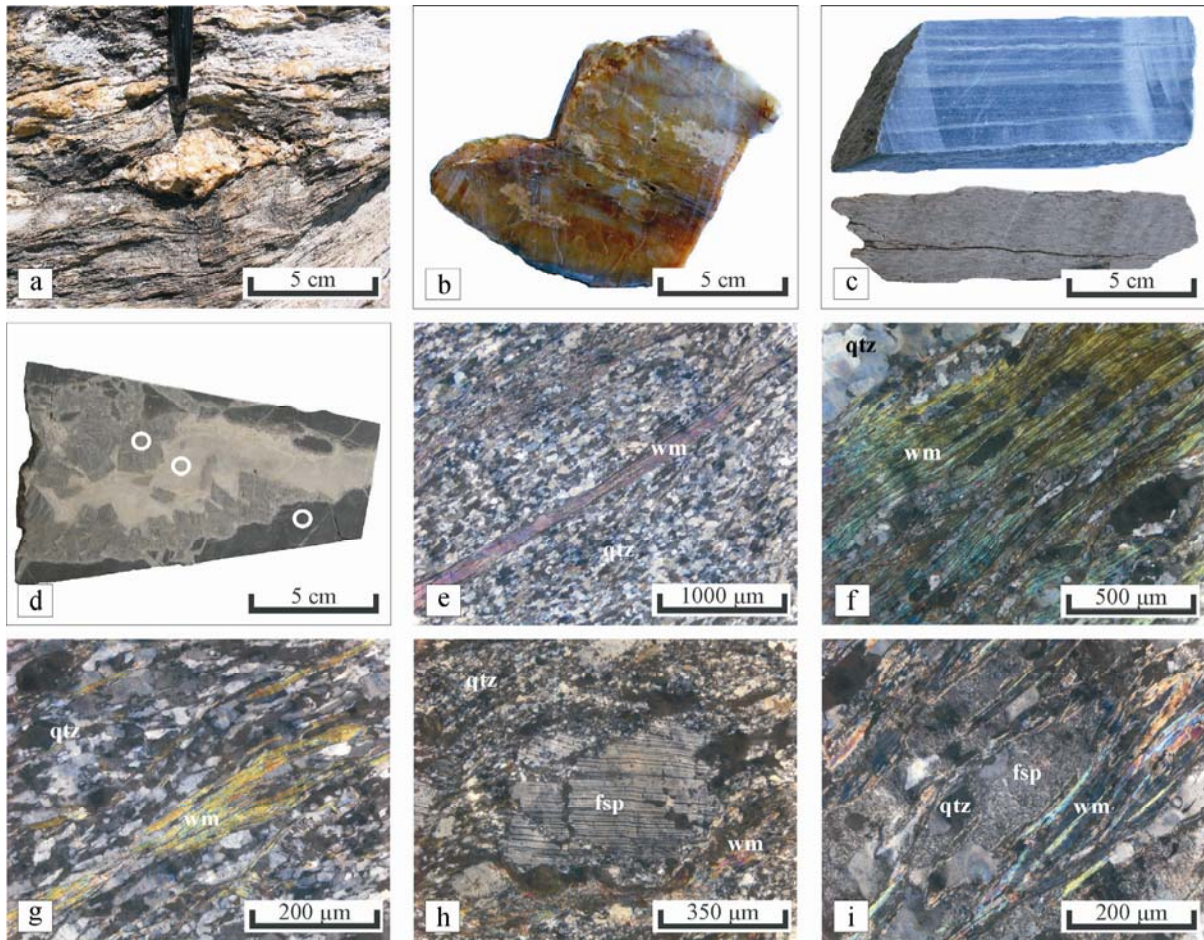


Figure 6.5: Outcrop, hand specimen and thin section images illustrating the different samples analysed for the present study (a) outcrop of foliation parallel prograde mobilisate at profile P-PG, (b) hand specimen of analyses sample B-8 (prograde mobilisate), (c) hand specimen of calcmylonite B-14 exhibiting tight foliation (upper part) and B-11 (qtz rich mylonite, upper plate, lower part of figure), (d) host rock (dark grey) and two vein generations of carbonatic sample 16b (lighter grey areas), white open dots indicate the position of microsampling for Sr isotope analyses, (e) thin section of sample C-15 showing strong foliation expressed by the alignment of white mica (wm), (f) thin section of sample B-11 also indicating deformation-induced recrystallization of white mica in the foliation, (g) thin section showing foliation parallel white mica with large variability of mica grain size (sample B-13), (h) thin section of sample C-12. Presence of some large feldspar clasts within dynamically recrystallized matrix as a possible reason for Sr-isotopic intermineral disequilibrium (see MSWD = 22), (i) thin section of sample J91 showing heavily sericitized feldspar minerals contributing to less complete isotopic reequilibration (see MSWD = 2185).

Sample 10c was taken from a shear zone within the upper plate basement at profile P-MO (Fig. 6.6). This sample represents a quartz-mica schist composed of qtz with bulging and subgrain rotation recrystallization, brownish bt, few heavily sericitized fs (pl with ab ~73 mole-%, an 27 mole-%), and minor ap. The tight foliation is formed by the alignment of fine-grained biotite and quartz-feldspar rich domains. In a few parts, larger biotite forms mica fish.

J91 represents a gneiss from the upper plate basement (Austroalpine nappe stack) sampled at profile P-JA (Fig. 6.6). It yields a paragenesis of qtz with subgrain rotation recrystallization, extremely sericitized fs (ab 68 mole-%, an 23 mole-%, or 9 mole-%) (Fig. 6.5i), ms (Si p.f.u. 3.12), and ap. Strong foliation is expressed by the alignment of white mica and quartz-feldspar domains.

Sample C-5 represents a Permian meta-volcanic rock exposed at the base of the

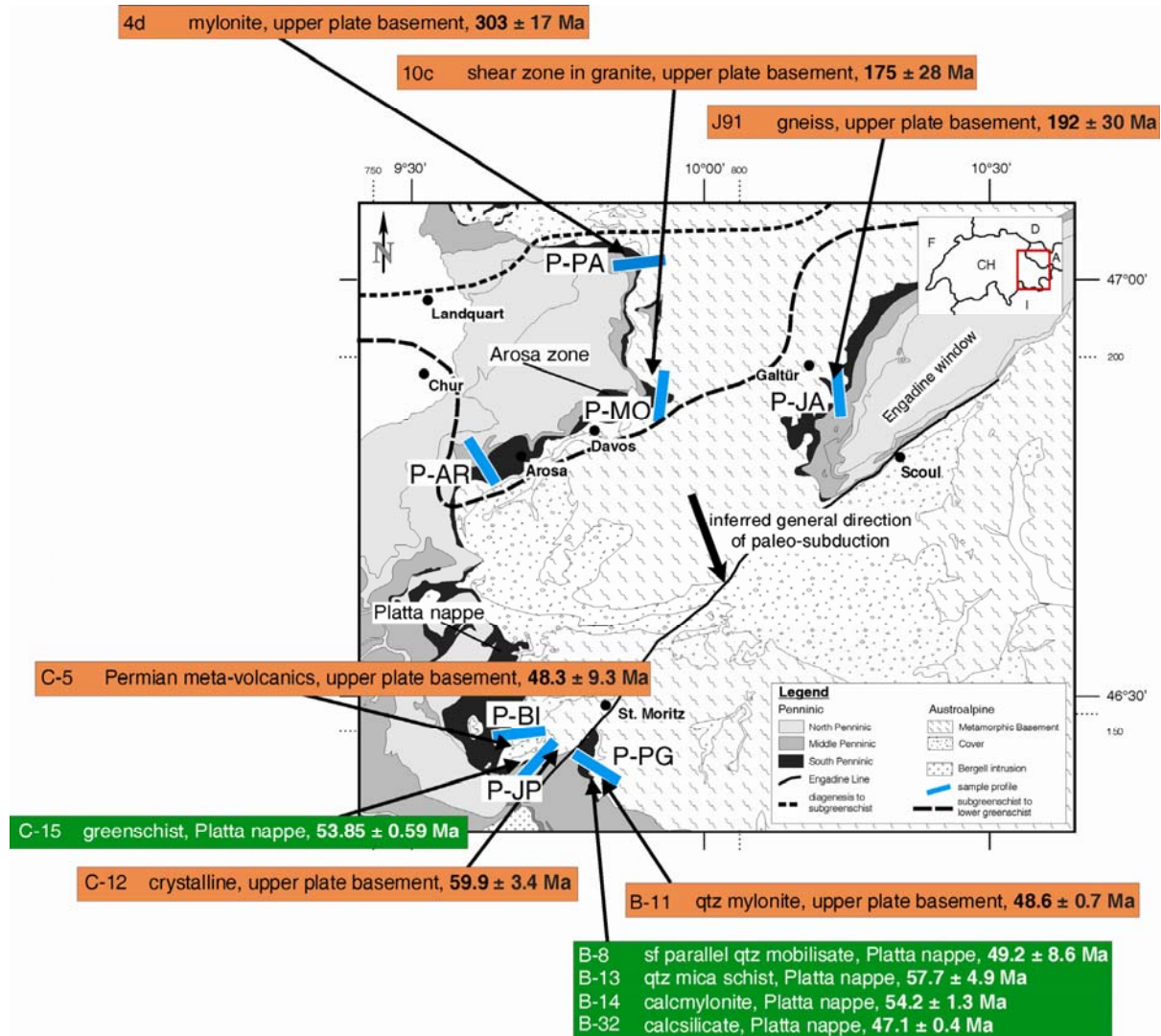


Figure 6.6: Tectonic map of the working area with profiles and sample positions for Rb/Sr geochronology, with new Rb/Sr deformation ages for the base of Austroalpine upper plate (orange) and the South Penninic subduction mélangé (green). Metamorphic isogrades redrawn after Frey et al. (1999).

upper plate at profile P-BI (Fig. 6.6). It is strongly deformed, and exhibits a closely spaced foliation. Its paragenesis is mainly composed of fs, ms, qtz showing undulose extinction, ap and minor mgt. In part, the mica rich layers are crenulated.

C-15 was sampled at profile P-JP (Fig. 6.6). It represents a quartz mica schist from the South Penninic mélangé, and contains qtz, which is partly recrystallized, fs, ms (Si p.f.u. 3.28) and minor ap. The tight foliation is defined by alternating quartz-feldspar and mica rich layers (Fig. 6.5e).

Sample C-12 represents a quartz mica schist from the base of the Austroalpine

upper plate at profile P-JP (Fig. 6.6). It is composed of qtz, almost pure ab, phg (Si p.f.u. 3.36) and ep. Quartz exhibits bulging recrystallization, whereas feldspar forms larger clasts in some parts (Fig. 6.5h).

Sample B-11 derives from the basal parts of the Austroalpine nappe stack at profile P-PG (Fig. 6.6). It represents a fine-grained quartz rich mylonite (Figs. 6.5c, f). The paragenesis is composed of qtz with subgrain rotation recrystallization, almost pure ab, phg (Si p.f.u. 3.41 – 3.43), and ap. The microtexture is characterized by the alternation of quartz-feldspar rich and mica

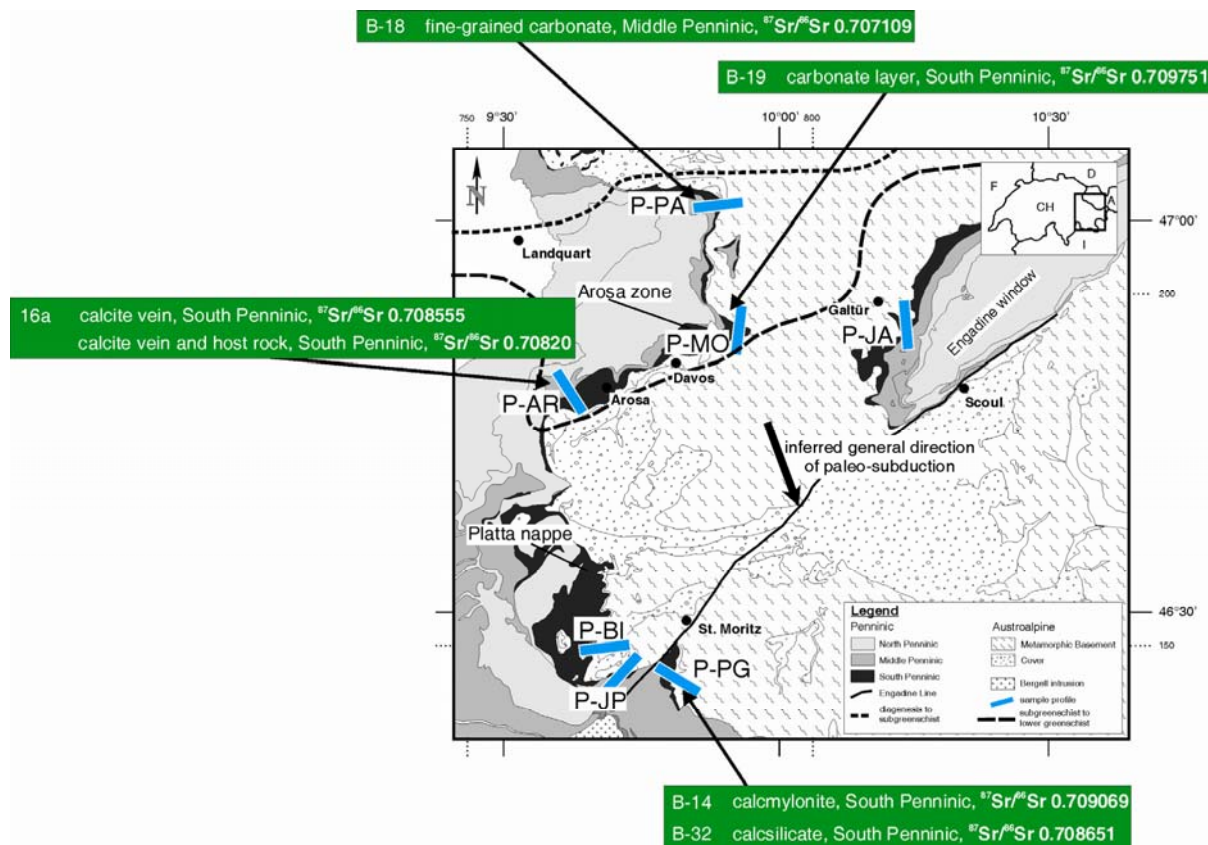


Figure 6.7: Tectonic map of the working area with profiles and sample positions for analyses of Sr isotope signatures, indicating $^{87}\text{Sr}/^{86}\text{Sr}$ values for marine (meta-) carbonates from the South Penninic subduction mélangé and the Middle Penninic domain. Metamorphic isogrades redrawn after Frey et al. (1999).

rich domains exhibiting a strong alignment of white mica (Fig. 6.5f).

Sample B-8 is a foliation-parallel quartz mobilisate (mineralized vein) taken from the South Penninic mélangé (Platta nappe) at profile P-PG (Figs. 6.5a, b, 6.6). It exhibits a blocky texture with coarse-grained qtz, finer-grained ab, ap and phg (Si p.f.u. ranging from 3.38 to 3.51). Quartz microstructure is dominated by subgrain rotation recrystallization.

The quartz-mica schist B-13 was taken from an outcrop of the South Penninic mélangé (Platta nappe) at profile P-PG (Fig. 6.6). It contains qtz, almost pure ab, phg (Si p.f.u. 3.42 – 3.44), and ap. Strong foliation is due to the alternation of quartz-feldspar rich and mica rich layers (Fig. 6.5g). Quartz microstructure is characterized by subgrain rotation recrystallization. Some larger feldspar

grains float within the finer-grained matrix. White mica is partly crenulated.

Sample B-14 was also sampled at profile P-PG, and represents a calcmylonite (Figs. 6.5c, 6.6). The sample was taken from the mylonitic outer parts of a large dolomite (?) clast (upper plate sedimentary cover) embedded within the South Penninic mélangé with its long axis apparently parallel to the main foliation. The rock is composed of cal (? dol), and ms. The strongly deformed sample exhibits an alternation of fine-grained and coarser-grained calcite, which highlights the foliation. Larger calcite grains exhibit tabular thick twins and rarely undulose extinction. Sparsely white mica grew along the foliation.

B-32 represents a calcsilicate from the South Penninic mélangé (Platta nappe) sampled at profile P-PG (Fig. 6.6). Its

paragenesis is composed of cal (with minor amounts of Fe, Mg and Mn), phg (Si p.f.u. ranging from 3.19 to 3.23), and ap. The strong foliation is caused by the alternation of mica, quartz and coarser grained calcite domains. Calcite shows tabular thick twins and subgrain rotation recrystallization in some cases. Quartz exhibits undulose extinction and incipient subgrain rotation recrystallization.

To sum up, samples for Rb/Sr isotopic dating yield very similar metamorphic conditions (middle to upper greenschist grade, as far as it can be constrained by the limited paragenesis), kinematic indicators (generally top-W) and microstructures (quartz showing bulging and subgrain rotation recrystallization, strongly aligned calcmylonites) for both the base of the upper plate Austroalpine domain and the South Penninic subduction mélange.

In addition, we sampled marine (meta-) carbonatic rocks from both the South Penninic mélange and the Middle Penninic (a few tens of meters below the base of the South Penninic subduction mélange) (Fig. 6.7) in order to conduct Sr isotope analyses for comparison with the Sr seawater evolution curve (cf. Howarth and McArthur 1997, McArthur et al. 2001). Sample B-18 represents a massive, nearly undeformed fine-grained carbonate from profile P-PA (Fig. 6.7). It was sampled from the Middle Penninic Sulzfluh unit for reference, because it was never part of the fossil South Penninic-Austroalpine plate interface zone. Sample B-19 is a carbonatic layer within a less deformed sediment pile at profile P-MO (Fig. 6.7). Samples 16a and 16b represent calcite-filled mineralized veins and the host rock (sample 16b black) (Fig. 6.5d). These samples were taken at profile P-AR (Fig. 6.7). Sample B-14 is a calcmylonite sampled at the rim of a carbonate clast of probably Triassic/Jurassic depositional age (Geological map of Switzerland, 1:500.000, 1980) embedded in the South Penninic mélange

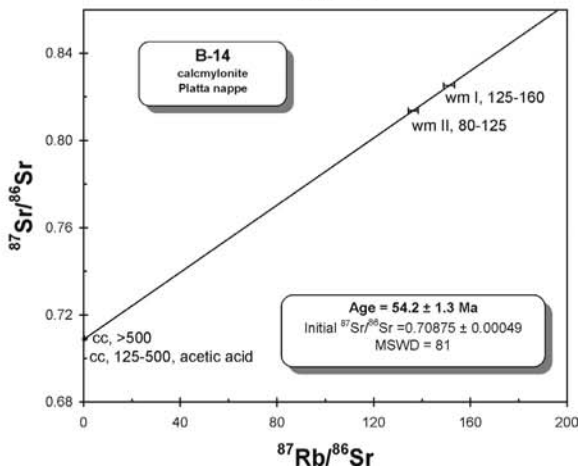
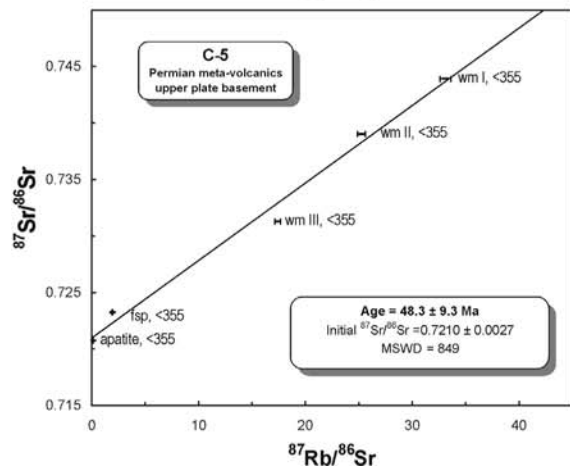
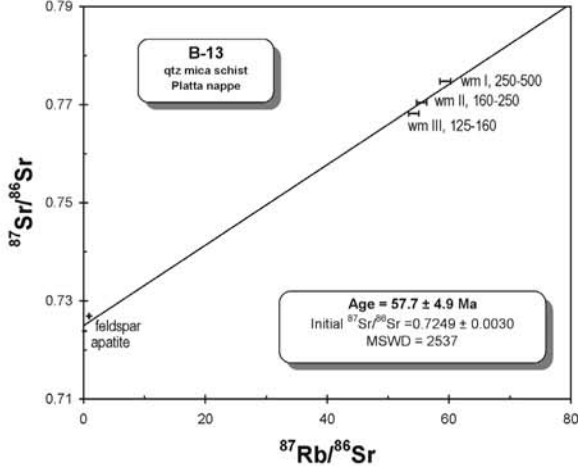
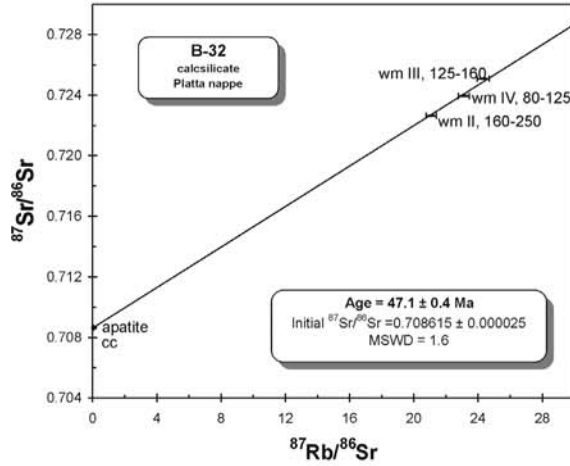
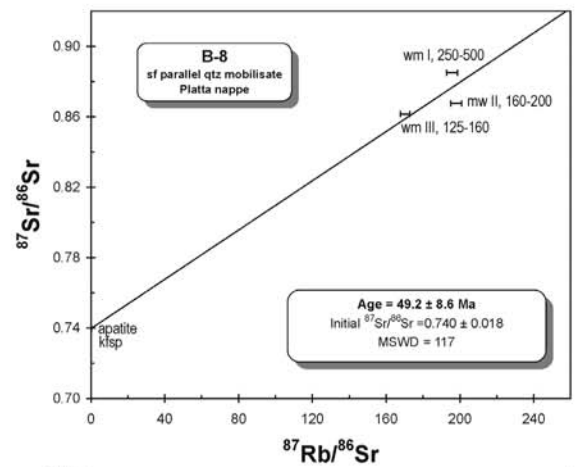
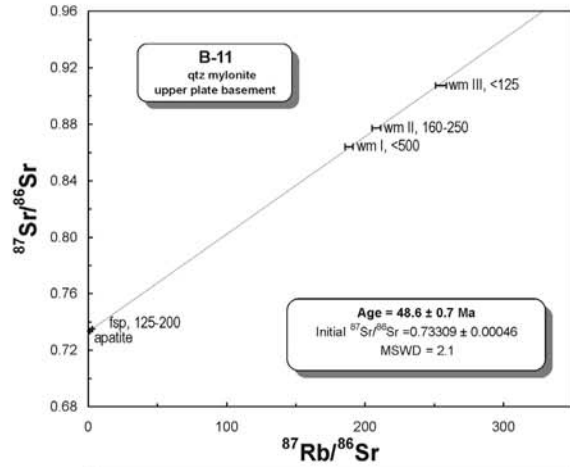
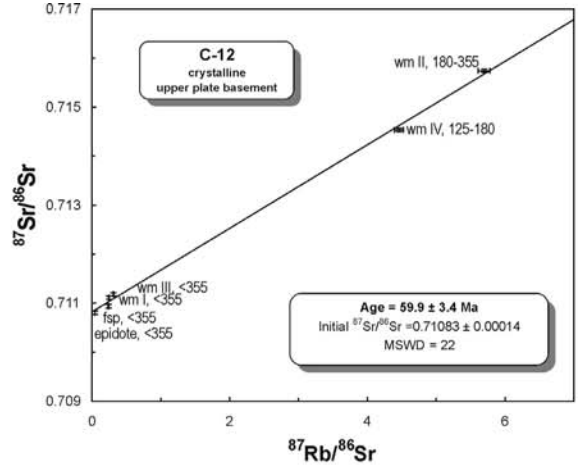
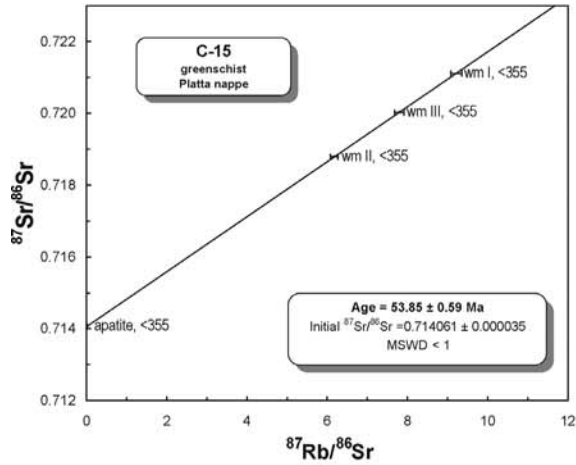
at profile P-PG (Figs. 6.5c, 6.7). B-32 represents a calcsilicate from the same profile (Fig. 6.7).

6.6. Results

6.6.1. Rb/Sr Data

Isotopic ages have been calculated using Rb/Sr isotope data for white mica, and cogenetic feldspar, apatite, calcite and epidote. We obtained well-defined isochron ages for three samples from the southern part of the working area, originating both from the basal parts of the Austroalpine upper plate and the South Penninic mélange. Sample C-15 (quartz mica schist, P-JP, South Penninic mélange) yielded a four-point isochron age of $53.85 \text{ Ma} \pm 0.59 \text{ Ma}$, sample B-11 (quartz rich mylonite, P-PG, Austroalpine) yielded a five-point isochron age of $48.6 \text{ Ma} \pm 0.7 \text{ Ma}$ (Fig. 6.8). The five-point isochron of sample B-32 (calcsilicate, P-PG, South Penninic mélange) resulted in a slightly younger age of $47.1 \pm 0.4 \text{ Ma}$ (Fig. 6.8). Additionally, for five samples from the upper plate and the South Penninic mélange, as well as for a quartz mobilisate we obtained correlations in Rb/Sr isochron plots which reveal minor apparent initial isotopic disequilibria between the analyzed mineral fractions (evident from elevated MSWD values of regression) (Fig. 6.8). Nevertheless, these samples give good hints on the age of their last important overprint. Sample C-5 (Permian meta-volcanic rock, P-BI, Austroalpine) resulted in an age of $48.3 \text{ Ma} \pm 9.3 \text{ Ma}$, based on a five-point correlation. A six-point

Figure 6.8: Internal mineral isochrons for samples from the South Penninic mélange and the Austroalpine upper plate. Analytical data are given in Table 1. Mineral abbreviations follow Kretz (1983). Grain size is indicated when different grain size fraction were analyzed.



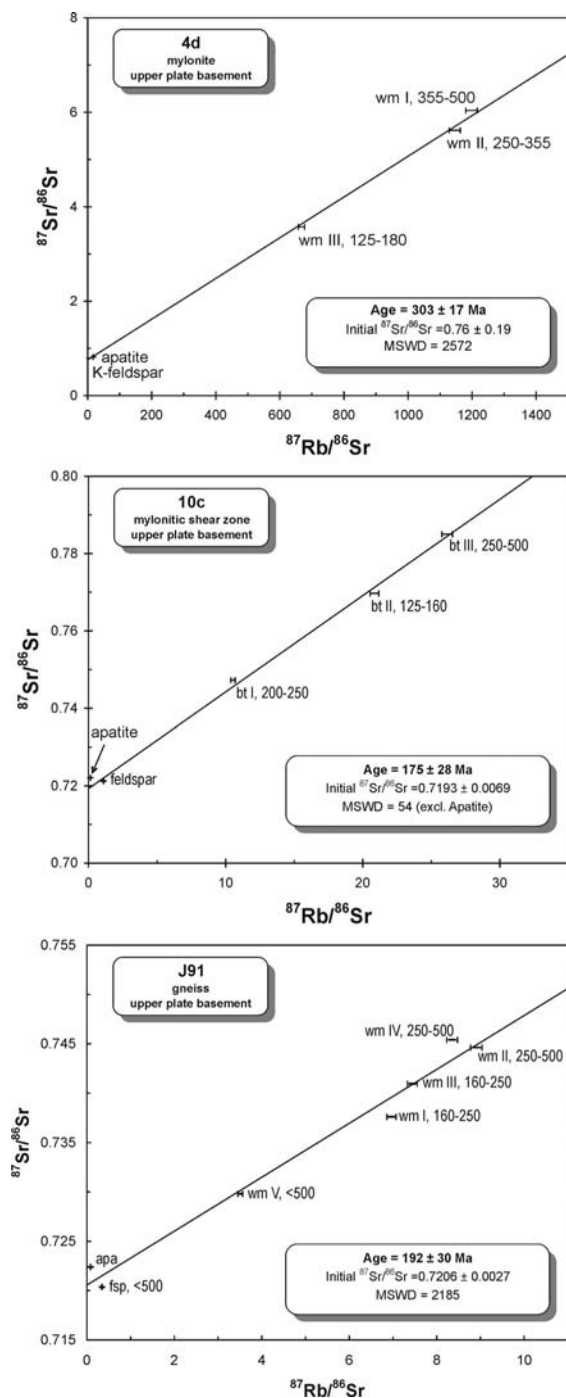


Figure 6.9: Rb/Sr mineral data for samples taken at the base of the crystalline upper plate in the northern part of the working area. Significance of isotopic disequilibria is discussed in the text. Analytical data are given in Table 1. Mineral abbreviations follow Kretz (1983). Grain size is indicated when different grain size fraction were analyzed.

correlation for sample C-12 (quartz mica schist, P-JP, Austroalpine) yielded an age value of $59.9 \text{ Ma} \pm 3.4 \text{ Ma}$. The quartz mobilisate B-8 (P-PG, South Penninic

mélange) resulted in a correlation based on five points corresponding to an age of $49.2 \text{ Ma} \pm 8.6 \text{ Ma}$. For sample B-13 (quartz mica schist, P-PG, South Penninic mélange), a five-point regression resulted in an age of $57.7 \pm 4.9 \text{ Ma}$. A four-point correlation was obtained for sample B-14 (calcmylonite, P-PG, South Penninic mélange) corresponding to an age of $54.2 \text{ Ma} \pm 1.3 \text{ Ma}$. In summary, there is a signal for a deformation process ending at $\sim 50 \text{ Ma}$.

Beside the above isotopic ages around 50 Ma, we obtained Rb/Sr mineral data pointing to considerably older, pre-Cretaceous events for some samples from the base of the crystalline upper plate (Austroalpine) in the northern part of the working area (Fig. 6.9). These samples are all characterized by Sr-isotopic disequilibria. Disequilibria are probably related to incomplete resetting of the mineral isotope systems due to incomplete deformation-induced recrystallization during younger overprints, for which indications are visible in thin sections (Fig. 6.5i). For sample 4d (mylonite, P-PA, the northernmost sample) regression of five Rb/Sr mineral data yielded $303 \text{ Ma} \pm 17 \text{ Ma}$ (Fig. 6.9). Sample 10c (mylonitic shear zone, P-MO) yields an apparent age of $175 \text{ Ma} \pm 28 \text{ Ma}$ ($n = 4$, MSWD = 54, excl. apatite; Fig 6.9). For sample J91 (gneiss, P-JA), regression of seven mineral data pairs points to an apparent age of $192 \text{ Ma} \pm 30 \text{ Ma}$ (Fig. 6.9).

6.6.2. Sr isotope signatures

Sr isotope signatures for our 8 marine (meta-) carbonate samples are plotted in Fig. 6.10, together with the Sr seawater evolution curve (cf. Howarth and McArthur 1997, McArthur et al. 2001). Two groups of samples can be distinguished, a) with $^{87}\text{Sr}/^{86}\text{Sr}$ of ~ 0.7071 , and b) with ratios above 0.708171. Group a) is represented by one sample from the

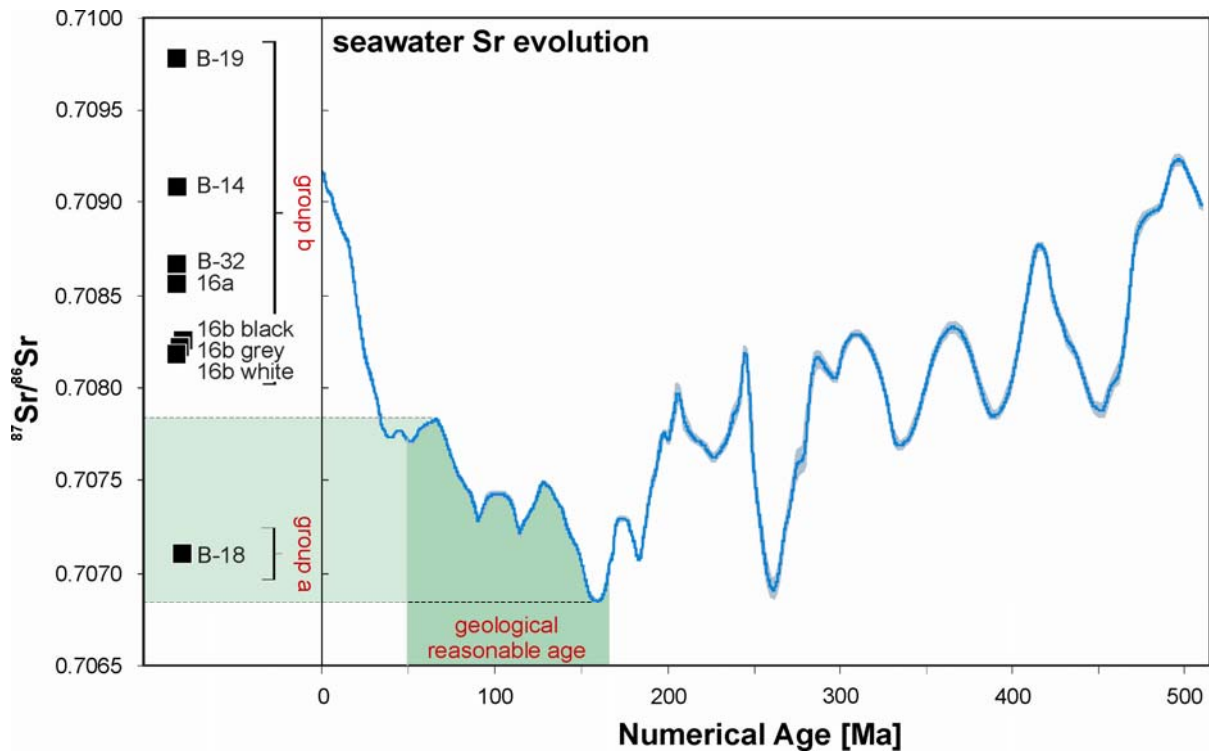


Figure 6.10: Diagram showing the Sr seawater evolution curve (McArthur et al. 2001) and the Sr data for 8 marine (meta-) carbonate samples. Two groups can be distinguished: Group a) was taken from the Middle Penninic unit, a few tens of meters below the base of the South Penninic subduction mélangé, and did not undergo deformation within the subduction channel. Its $^{87}\text{Sr}/^{86}\text{Sr}$ ratio indicates carbonate deposition during the Upper Jurassic, and no evidence for later alteration. Group b) comprises samples taken from the subduction channel with elevated $^{87}\text{Sr}/^{86}\text{Sr}$ ratios, incompatible with the Sr seawater ratios during the geologically reasonable carbonate deposition interval (dark green area).

Middle Penninic Sulzfluh unit (B-18), which did not undergo deformation or recrystallization within the fossil South Penninic-Austroalpine plate interface zone. Its $^{87}\text{Sr}/^{86}\text{Sr}$ ratio is 0.707109. Group b) comprises samples taken from the South Penninic mélangé with $^{87}\text{Sr}/^{86}\text{Sr}$ ratios between 0.708171 and 0.709751, which are consistently higher than $^{87}\text{Sr}/^{86}\text{Sr}$ ratios of geologically reasonable (Jurassic to Paleocene) segments of the Sr seawater evolution curve (Fig. 6.10, Table 2). Sample B-19 yields a Sr isotope value of 0.709751; sample 16a has an $^{87}\text{Sr}/^{86}\text{Sr}$ signature of 0.708555. $^{87}\text{Sr}/^{86}\text{Sr}$ ratios of sample 16b (16b black, 16b grey, 16b white, Fig. 6.5d) are analytically indistinguishable at around 0.70820. Sample B-14 exhibits an $^{87}\text{Sr}/^{86}\text{Sr}$ ratio of 0.709069, whereas sample B-32 shows an $^{87}\text{Sr}/^{86}\text{Sr}$ ratio of 0.708651.

6.7. Discussion

6.7.1. Rb/Sr ages

To determine the absolute timing of penetrative deformation within the South Penninic mélangé and the basal parts of the Austroalpine nappe stack we used Rb/Sr geochronology on pervasively deformed rocks from both tectonic units. In addition, we dated one mineralized vein running subparallel to the foliation within the South Penninic mélangé to relate the formation of these vein systems to the overall deformation.

As outlined above, all samples are taken from outcrops reflecting a general top-W direction of tectonic transport (see Chapter 6.2.3.), although they may exhibit relics of former deformational stages, or may have

Table 1. Rb/Sr analytical data.

sample	material	Rb [ppm]	Sr [ppm]	$^{87}\text{Rb}/^{86}\text{Sr}$	$^{87}\text{Sr}/^{86}\text{Sr}$	$^{87}\text{Sr}/^{86}\text{Sr} \ 2s_m$ (%)
<i>4d (mylonite; 303 ± 17 Ma; MSWD = 2572, $Sr_i = 0.76 ± 0.19$)</i>						
PS1355	wm I, 355-500	896	3.29	1198	6.038448	0.0078
PS1354	wm II, 250-355	885	3.31	1146	5.616657	0.0050
PS1353	wm III, 125-180	783	4.35	668	3.572638	0.0116
PS1426	fsp	197	33.7	17.1	0.820349	0.0030
PS1356	apatite	9.67	91.7	0.307	0.797647	0.0018
<i>10c (mylonite; 175 ± 28 Ma; MSWD = 54 (excl. ap), $Sr_i = 0.7193 ± 0.0069$)</i>						
PS1376	bt I, 200-250	230	63.3	10.5	0.747277	0.0018
PS1375	bt II, 125-160	242	33.8	20.9	0.769687	0.0038
PS1372	bt III, 250-500	251	27.9	26.2	0.785026	0.0016
PS1374	fsp	34.4	90.7	1.10	0.721254	0.0020
PS1373	apatite	8.01	171	0.136	0.722105	0.0014
<i>J91 (gneiss; 192 ± 30 Ma; MSWD = 2185, $Sr_i = 0.7206 ± 0.0027$)</i>						
PS1511	wm I, 160-250	188	78.4	6.97	0.737618	0.0014
PS1512	wm II, 250-500	194	63.3	8.90	0.744635	0.0012
PS1513	wm III, 160-250	189	73.6	7.44	0.740965	0.0014
PS1514	wm IV, 250-500	186	64.7	8.35	0.745408	0.0014
PS1515	wm V, <500	148	122	3.51	0.729797	0.0016
PS1517	fsp, <500	70.9	599	0.343	0.720367	0.0016
PS1516	apatite	6.21	217	0.0829	0.722397	0.0018
<i>C-5 (Permian metavolcanic rock; 48.3 ± 9.3 Ma; MSWD = 849, $Sr_i = 0.7210 ± 0.0027$)</i>						
PS1505	wm I <355 µm	282	24.7	33.1	0.743921	0.0014
PS1506	wm II <355 µm	260	29.9	25.2	0.739032	0.0014
PS1507	wm III <355 µm	192	32.0	17.4	0.731291	0.0012
PS1510	fsp <355 µm	318	480	1.92	0.723244	0.0014
PS1509	apatite	12.8	312	0.119	0.720741	0.0016
<i>C-15 (quartz mica schist; 53.85 ± 0.59 Ma; MSWD < 1, $Sr_i = 0.714061 ± 0.000035$)</i>						
PS1518	wm I <355 µm	110	34.4	9.22	0.721113	0.0016
PS1519	wm II <355 µm	48.0	22.5	6.17	0.718788	0.0016
PS1520	wm III <355 µm	78.4	29.1	7.80	0.720022	0.0014
PS1521	apatite	10.3	3194	0.00935	0.714068	0.0018
<i>C-12 (quartz mica schist; 59.9 ± 3.4 Ma; MSWD = 22, $Sr_i = 0.71083 ± 0.00014$)</i>						
PS1490	wm I <355 µm	12.8	151	0.247	0.711112	0.0014
PS1491	wm II 180-355 µm	274	139	5.70	0.715743	0.0014
PS1493	wm III <355 µm	11.9	110	0.313	0.711180	0.0016
PS1494	wm IV 125-180 µm	179	116	4.46	0.714533	0.0014
PS1496	fsp <355 µm	3.42	41.3	0.239	0.710940	0.0014
PS1492	epi <355 µm	19.3	1318	0.0424	0.710808	0.0012
<i>B-11 (qtz mylonite; 48.6 ± 0.7 Ma; MSWD = 2.1, $Sr_i = 0.73309 ± 0.00046$)</i>						
PS1405	wm I <500 µm	533	8.31	188	0.864115	0.0020
PS1404	wm II 160-250 µm	549	7.76	208	0.877306	0.0020
PS1403	wm III <125 µm	557	6.45	255	0.907476	0.0030
PS1427	fsp 125-200 µm	27.2	27.3	2.90	0.735181	0.0062
PS1378	apatite	445	1301	0.991	0.733649	0.0012
<i>B-8 (foliation parallel qtz mobilisate; 49.2 ± 8.6 Ma; MSWD = 117, $Sr_i = 0.740 ± 0.018$)</i>						
PS1369	wm I 250-500 µm	515	7.74	196	0.884915	0.0022
PS1368	wm II, 160-200 µm	541	8.03	198	0.867532	0.0020
PS1367	wm III 125-160 µm	453	7.81	170	0.861505	0.0036
PS1371	kfsp >500 µm	4.00	55.0	0.211	0.739813	0.0014
PS1370	apatite	2.15	1157	0.00539	0.739322	0.0018
<i>B-13 (qtz mica schist; 57.7 ± 4.9 Ma; MSWD = 2537, $Sr_i = 0.7249 ± 0.0030$)</i>						
PS1409	wm I 250-500 µm	479	23.5	59.4	0.774758	0.0024
PS1408	wm II 160-250 µm	477	25.0	55.5	0.770414	0.0020
PS1407	wm III 125-160 µm	461	24.7	54.2	0.768190	0.0043
PS1428	fsp 90-160 µm	9.88	31.8	0.900	0.726888	0.0016
PS1410	apatite	6.29	1303	0.0140	0.723852	0.0014
<i>B-14 (calcmylonite; 54.2 ± 1.3 Ma; MSWD = 81, $Sr_i = 0.70875 ± 0.00049$)</i>						
PS1412	wm I 125-160 µm	149	2.89	151	0.825256	0.0022
PS1411	wm II 80-125 µm	73.4	1.57	136	0.813684	0.0062
PS1359	cc >500 µm	32.6	294	0.321	0.709157	0.0014
PS1377	cc 125-500 µm	2.06	115	0.0520	0.708628	0.0016
<i>B-32 (calcsilicate; 47.1 ± 0.4 Ma; MSWD = 1.6, $Sr_i = 0.708615 ± 0.000025$)</i>						
PS1415	wm II 160-250 µm	283	38.9	21.1	0.722641	0.0012
PS1414	wm III 125-160 µm	333	39.7	24.3	0.725086	0.0014
PS1413	wm IV 80-125 µm	182	22.9	23.1	0.723945	0.0014
PS1429	cc >500 µm	6.71	308	0.0631	0.708651	0.0016
PS1417	apatite	1.67	477	0.0101	0.708629	0.0016

Table 2. Rb/Sr analytical data, carbonates and metacarbonates.

sample	material	weight (mg)	Rb (ppm)	Sr (ppm)	$^{87}\text{Rb}/^{86}\text{Sr}$	$^{87}\text{Sr}/^{86}\text{Sr}$	$^{87}\text{Sr}/^{86}\text{Sr}$ $2\sigma_m$ (in %)
16a	carbonate	10.5	1.03	176	0.0169	0.708555	0.0012
16b black	host rock carbonate	8.5	2.21	106	0.0602	0.708246	0.0012
16b grey	vein generation I	9.4	0.04	315	0.00039	0.708200	0.0014
16b white	vein generation II	10.0	0.29	1245	0.00068	0.708171	0.0016
B-14	calcmylonite	8.3	0.36	345	0.00300	0.705000	0.0014
B-18	carbonate Sulzfluh	8.8	0.09	198	0.00135	0.707109	0.0016
B-19	carbonate	11.5	2.85	427	0.0193	0.709751	0.0014
B-32	calcsilicate	3.8	6.71	308	0.0631	0.708651	0.0016

been exposed to later overprints. The analyses of Rb/Sr data for the different samples resulted in 2 age groups (Fig. 6.11a). The first group is exclusively comprised of samples from the base of the upper plate Austroalpine nappe stack. Here, the oldest apparent age of $303 \text{ Ma} \pm 17 \text{ Ma}$ (sample 4d, Fig. 6.9) is within the range of ‘Variscan’ ages known from the Austroalpine of the region (cf. Thöni 1999 for review), while the data for sample J91 (disequilibria; poorly constrained apparent age of $192 \pm 30 \text{ Ma}$, Fig. 6.9) might reflect partial resetting of pre-Alpine signatures, probably by Alpine-age overprints. The fact that the apparently ‘younger’ sample originates from a more southern (deeper) position within the fossil plate interface is consistent with the observed increasing intensity of Alpine imprints on textures and mineral assemblages towards the S (see Chapter 4). A low degree of Alpine impact on the northernmost sample correlates with only sub-greenschist-facies Alpine imprint, whereas the more strongly affected sample was located already in a lower greenschist facies Alpine environment (Figs. 6.6, 6.11a), an observation pointing to more effecting resetting of the isotope system by deformation at higher metamorphic conditions. Sample 10c from a mylonitic

shear zone within the upper plate resulted in an age of $175 \text{ Ma} \pm 28 \text{ Ma}$ (Fig. 6.9). It remains unclear whether this (biotite-based) age value may also reflect the incomplete reset of Variscan isotope signature by Alpine deformation. It is worth noting that this age is in accordance to published age data for the breakup of the continent finally leading to the opening of the Alpine Tethys in between Europe and Africa (e.g. Schmid et al. 2004 and references therein). The here sampled shear zone may, therefore, alternatively represent a deformation zone related to the above Jurassic continental extension and breakup (e.g. Froitzheim and Rubatto 1998, Manatschal et al. 2006 for the interpretation of the ocean-continent transition in the Swiss Alps).

The second group comprising samples from both the base of the Austroalpine nappe stack and the South Penninic mélange in the southern part of the working area, resulted in ages roughly around 50 Ma (Fig. 6.11a). For the samples from the basal parts of the upper plate we interpret these ages to reflect the final stages of mylonitization-related isotopic reequilibration from penetrative Alpine deformation, under greenschist grade conditions (at least close to the boundary to

the underlying South Penninic *mélange*). There is a striking similarity between the deformation ages calculated for the basal parts of the upper plate, and for the South Penninic *mélange*, in the southern part of the study area (Fig. 6.11b). We therefore interpret the ages obtained for the South Penninic *mélange* to reflect the same deformation-induced recrystallization as observed in the upper plate samples. It appears that deformation along the plate interface zone of the South Penninic *mélange* and the Austroalpine nappe stack (and affecting rocks from both tectonic units) occurred over a prolonged period, at least over a time span bracketed by our isochron age data (53.85 ± 0.59 Ma to 47.1 ± 0.4 Ma). Possibly even somewhat earlier increments of deformation are recorded by the samples C-12 (Fig. 6.8) and B13 (Fig. 6.8). These samples show higher apparent ages (59.9 ± 3.4 and 57.7 ± 4.9 Ma, respectively), combined with positive correlations between white mica grain sizes and apparent ages (e.g. sample B13: large white mica crystals plotting above, and smaller white micas below the regression line, Fig. 6.8). This grain size – age correlation reflects some kind of isotopic inheritance. It is consistent with protracted deformation, with incomplete isotopic resetting of early-recrystallized grains during the latest stages of deformation. Finally, there is no hint in the dataset to any ductile overprint postdating the Lower Eocene (~50 Ma) record of waning deformation.

The dated foliation parallel prograde mobilisate (B-8) resulted in an (imprecisely constrained) apparent age of 49.2 ± 8.6 Ma (Fig. 6.8), pointing to the activity of fluids along the active paleosubduction zone. Pseudotachylytes from the base of the Austroalpine upper plate in the northern part of the working area has previously been dated by Thöni (1988) to ~75 Ma (Figs. 6.11a, b). Own Ar/Ar data point to pseudotachylyte formation within a prolonged time frame

of 60 Ma to 80 Ma (see Chapter 5). We interpreted the formation of pseudotachylyte to be related to the subduction of the South Penninic *mélange* underneath the Austroalpine upper plate (Chapter 5), giving another hint for the time frame of subduction-related deformation. Material accreted to the base of the South Penninic subduction *mélange* (i.e. the Middle Penninic domain) yield synkinematic white mica ages around 38 Ma (Markley et al. 1995), which point to subduction related deformation at that time in the footwall of the South Penninic subduction *mélange* (Fig. 6.11a). In summary, our Rb/Sr isotopic data provide the first precise geochronological constraints on the end of subduction related deformation along the South Penninic-Austroalpine suture zone in the Eastern Swiss Alps, i.e. on the abandonment of this paleosubduction interface.

One fact has to be pointed out: The deformational and isotopic record of a subduction channel is persistently renewed due to continuous processes such as sediment subduction, deformation, and tectonic erosion. Only when material finally leaves the active parts of the subduction channel and becomes accreted to the base of the hanging wall, the deformational and isotopic record can be preserved. Deformation-induced isotopic resetting during accretion of material to the base of the upper plate is caused by permanent strain accumulation due to velocity gradient between material flow within the channel and the upper plate. Depending on the degree of coupling between upper and lower plate, deformation and consequently a zone of deformation-induced isotopic resetting may even penetrate into the base of the overriding plate. As outlined above, we interpret our Rb/Sr age data as indicating the removal of material out of the active parts of the subduction channel and as dating the abandonment of the South

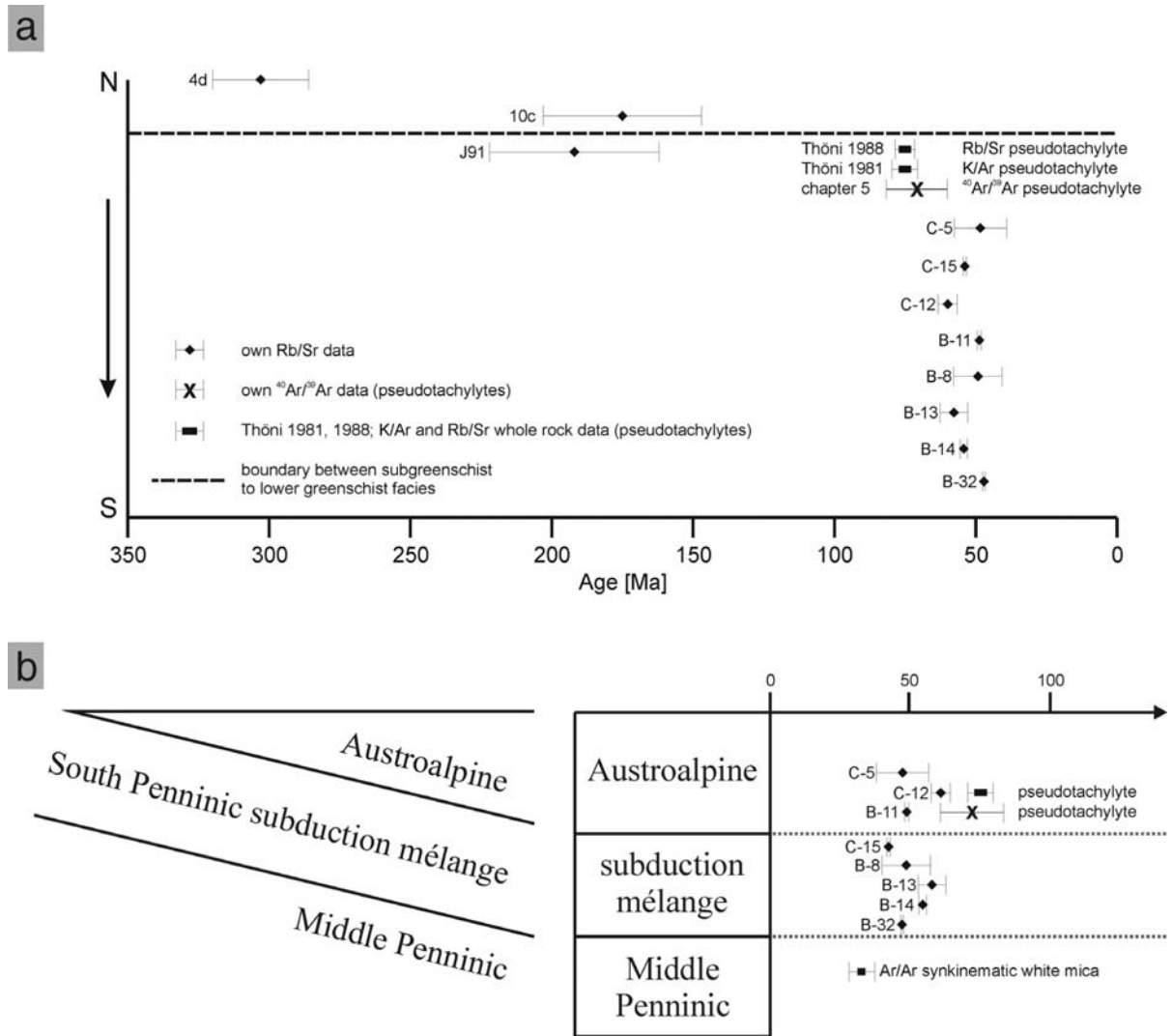


Figure 6.11: a) Distribution of Rb/Sr age data from N to S. There is a clear subdivision into two group of ages, the first group > 175 Ma and the second group at ~ 50 Ma. Position of metamorphic isograds taken from Frey et al. (1999). b) Position of own Rb/Sr data relative to either the Austroalpine upper plate or the South Penninic mélangé showing the similarity of deformation ages obtained for both units. Additionally, Rb/Sr ages (Thöni 1988), K/Ar ages (Thöni 1981), and own $^{40}\text{Ar}/^{39}\text{Ar}$ ages (see Chapter 5) for pseudotachylytes formation within the basal part of the upper plate, as well as Ar/Ar synkinematic white mica ages for the Middle Penninic domain (Markley et al. 1995) are indicated.

Penninic-Austroalpine suture zone at around 50 Ma. This is in accordance with results of Liu et al. (2001), dating the final emplacement of Austroalpine units onto the Penninic domain at around 55-50 Ma using Ar/Ar muscovite ages for the area east of the Tauern window. Furthermore, Liu et al. (2001) associate the Cretaceous to Early Tertiary deformation within the lower part of the Austroalpine nappe complex with top-WNW directed transport, which is well comparable to our

structural data (see Chapter 2.3.) pointing to a general top-W direction of tectonic transport during the Cretaceous to Early Eocene subduction-related deformation.

6.7.2. Sr isotopes

We studied the Rb/Sr isotope signature of 8 originally marine (meta-) carbonate samples from the fossil plate interface zone to get information about both their age

relationships and possible interaction with either crustal or mantle derived fluids. The carbonates are believed to have formed in a seawater environment (South Penninic ocean), and thus should record the syn-precipitational $^{87}\text{Sr}/^{86}\text{Sr}$ ratio of seawater, given that no later, post-depositional fluid-rock interaction occurred. The Sr-isotopic ratio of seawater is known to vary with time (e.g. Wickman 1948, Gast 1955), so that Sr isotopic compositions of seawater precipitates (e.g. biogene carbonates) may directly be converted to absolute age information ('strontium isotope stratigraphy', cf. Howarth and McArthur 1997, McArthur et al. 2001). For reliable age information to be extracted from Sr isotope signatures, several preconditions have to be met, namely that no detrital components contaminate the seawater precipitates, that the Sr isotopic signature is not changed by in-situ decay of Rb, and that no secondary exchange of Sr with external fluids ever occurred. Monitoring of Rb contents and Rb/Sr ratios and microscopic examination of the studied samples has shown that siliciclastic detrital components are virtually absent, and Rb/Sr ratios are very low (Table 2), indicating that in-situ radiogenic ingrowth of ^{87}Sr in the carbonate samples is negligible. Therefore, the Sr isotope data either provide information on primary Sr isotopic signatures or give hints to possible interaction and Sr exchange with fluids during syn-subduction metamorphism.

We distinguished the analyzed samples into two groups (see Chapter 6.7.2). Group a) yields Sr isotope values around 0.7071 for a reference sample from the Middle Penninic (Sulzfluh, close to the base to the overlying South Penninic subduction mélange). This value corresponds with either a Permian or Upper Jurassic Sr isotope stratigraphy age (Fig. 6.10). This fits well with geological constraints indicating an Upper Jurassic (Malm) age (Geological map of Switzerland, 1:500.000, 1980) of marine carbonate

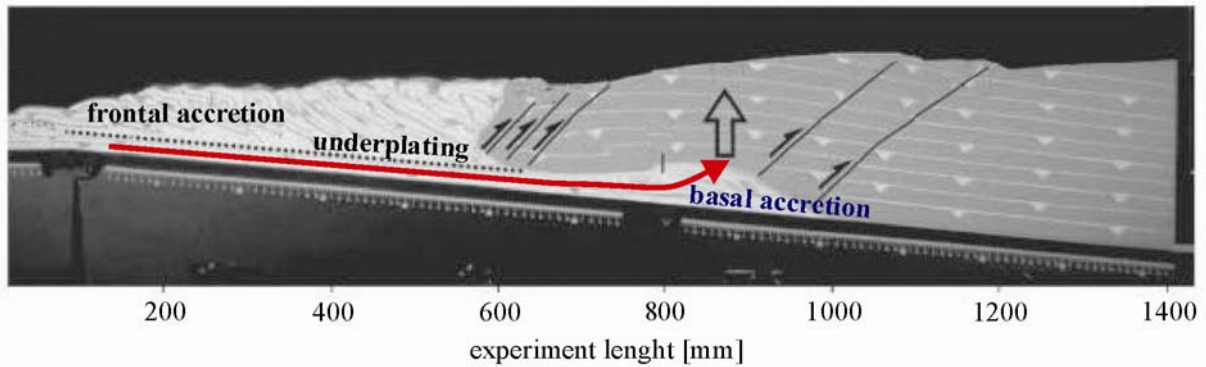
deposition on top of the submerged Middle Penninic micro-continent. There is no evidence for influence of fluids or deformation-related recrystallization, which altered the $^{87}\text{Sr}/^{86}\text{Sr}$ subsequently. The isotopic data thus confirm the Malm age of the rock, and show that it escaped from subduction-related overprints.

Group b) yielded elevated Sr isotope signature (>0.708171) for samples from the South Penninic mélange. Similar $^{87}\text{Sr}/^{86}\text{Sr}$ ratios in seawater prevailed only in Ordovician, Permian, or Miocene to Recent times, and all these potential deposition intervals are incompatible with the geological setting of the carbonates. This suggests a significant interaction of the carbonates of this group with fluids carrying Sr with $^{87}\text{Sr}/^{86}\text{Sr} > 0.708171$, i.e., with fluids interacting with old continental crustal material. Most likely, the dominant source for the syn-subduction fluids, which altered the samples, is prograde dehydration of continent-derived sediments during subduction. Contributions to the subduction fluids from other sources, like from dehydration of oceanic crust, cannot be ruled out, but must have been minor due to the low $^{87}\text{Sr}/^{86}\text{Sr}$ ratios expected for such fluids. Such fluids would range between MORB values around 0.703 and Paleogene seawater values of < 0.7078 , i.e. their isotopic composition would be in marked contrast with the compositions observed in the mélange samples.

6.7.3. Exhumation of the South Penninic-Austroalpine plate interface zone

The suture zone between the South Penninic mélange (Arosa zone, Platta nappe) and the Austroalpine nappe stack does not exhibit a clear metamorphic contrast between hanging wall and footwall (Figs. 6.1, 6.6, 6.7) (e.g. Nievergelt et al. 1996). In terms of possible exhumation mechanisms this would argue for erosion as the principle driving force (see discussion in Froitzheim et al. 2003).

a Sandbox model



b Schematic drawing of underplated Middle Penninic units (~55-45 Ma)

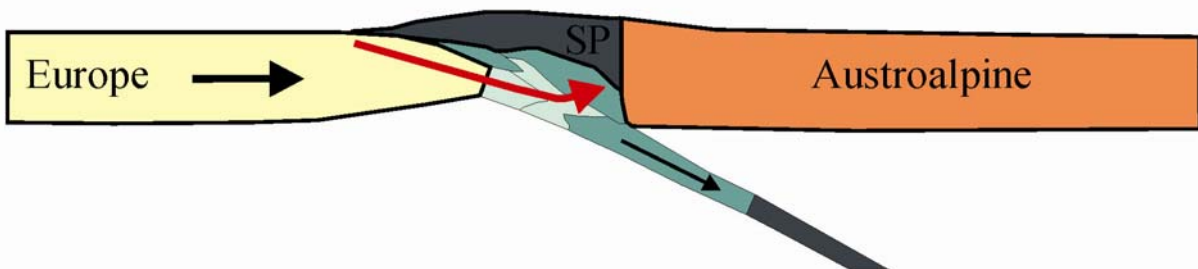


Figure 6.12: (a) Sandbox model indicating processes of frontal and basal accretion (modified after Glodny et al. 2005). (b) Schematic drawing of underplating of the Middle Penninic micro-continent at around 55 Ma to 45 Ma (redrawn after von Blanckenburg and Davies (1995).

However, differential exhumation of the suture zone (diagenetic to lowest greenschist facies conditions in the northern part, roughly upper greenschist facies conditions towards the south, Figs. 6.6, 6.7, e.g. Chapter 4), the observation of underfilled foreland basins during the initial time of subduction (prior to Oligocene) reported by Ford et al. (2006), as well as the initial onset of major sediment input into the foreland basins between 31 Ma and 20 Ma due to erosion of the rapidly emerging orogen (von Eynatten et al., 1999; Schlunegger et al., 1998; Spiegel et al., 2000; Liu et al., 2001, Kuhlemann et al. 2006) would favor additional processes than erosion, which contributed to the exhumation at least prior to the Oligocene.

In addition to erosion, we propose the accretion of subducted material to the base of the upper plate (Austroalpine nappes) as the key mechanism accounting for the exhumation of the studied suture zone. Such a process is theoretically predicted from numerical and analogue modeling (Fig. 6.12a) (Allemand and Lardeaux 1997, Kukowski et al. 2002, Lohrmann 2002). This would also require no metamorphic contrast between hanging wall and footwall. Basal accretion would lead to basal wedge growth by antiformal stacking of the subducted and underplated material (Glodny et al. 2005, and references therein). Ongoing basal accretion roughly at the same position in space would lead to extension of the accreted material simply caused by doming. Following a principle particle path down the subduction plate interface would

be as follows (Fig. 6.12a): 1. Entering the subduction zone at the tip of the accretionary wedge, 2. Passing down the plate interface zone within the subduction channel, and prograde metamorphism, 3. Accretion to the base of the upper plate, removal from the active subduction channel, and thereby caused penetrative deformation due to velocity contrast of particle flow within the subduction channel and the upper plate, 4. Uplift, extension and retrogressive metamorphism due to ongoing basal accretion. The hypothetical sample would receive its isotopical and structural record when it finally left the active subduction channel and became accreted to the base of the hanging wall.

Von Blanckenburg and Davies (1995) suggest the underplating of continental Penninic material (most likely the Middle Penninic micro-continent) below the overriding plate in a time span between 55 Ma and 45 Ma (Fig. 6.12b). Our Rb/Sr age data are in line with these suggestions. They clearly show the end of deformation along the South Penninic-Austroalpine suture zone at roughly 50 Ma, which should be caused by the locking of the South Penninic subduction zone by the incoming Middle Penninic micro-continent. This might have transferred the zone of active deformation further into the footwall, making the South Penninic subduction mélange a part of the upper plate, which subsequently overrides the Middle Penninic domain.

6.7.4. Gosau group – additional evidence for abandonment of the Alpine subduction zone

Additional constraints for timing of subduction and for the subduction-associated mass transfer mode are given by Wagneich (e.g. 1991, 1995) referring to the initial development of the Late Cretaceous Gosau basins as slope basins at the northward deepening slope at the front of

the orogenic wedge (Wagneich and Krenmayr 2005). According to these authors the Gosau basins represent synorogenic sedimentation along a broad transform zone, and are the consequence of oblique subduction of the South Penninic ocean underneath the Austroalpine nappe stack starting in the Late Cretaceous with dextral transpression and strike-slip faulting. The Gosau basins comprise a stratigraphic record from the Upper Turonian to the Eocene evolving from terrestrial and shallow marine deposits (Lower Gosau subgroup) into deep marine sediments (Upper Gosau subgroup). The Upper Gosau subgroup is associated with tectonic erosion and a thereby caused large scale subsidence pulse during the Late Cretaceous to the Eocene (e.g. Wagneich 1991). The change from an accretive to a tectonically erosive margin with the onset of Gosau group sedimentation might be due to the subduction of a SW-NE trending topographic high (Wagneich 1995). This explains the observed time shift in uplift, deformation and subsidence from northwest to southeast throughout the Gosau group depocenters (Fig. 6.13, Wagneich 1995). According to Wagneich (1995) this observation is comparable to active convergent plate margins, where seamount chains (e.g. Tonga Trench, Balance et al. 1989) or spreading ridges (e.g. Peru-Chile trench, Nelson and Forsythe 1989) collide obliquely with the upper plate. Another resemblance to active convergent plate margins is reported by Sanders and Höfling (2000). According to these authors the carbonatic depositional systems of the Gosau group are similar with respect to physiographic settings, scale, and facies to Holocene mixed siliciclastic-carbonate environments in active convergent settings. In addition, subsidence curves for the Miocene to Recent record of the erosive Japan margin are well comparable in shape, magnitude and duration to the Upper Gosau subgroup subsidence curves (von Huene and Lallemand 1990, Wagneich 1995).

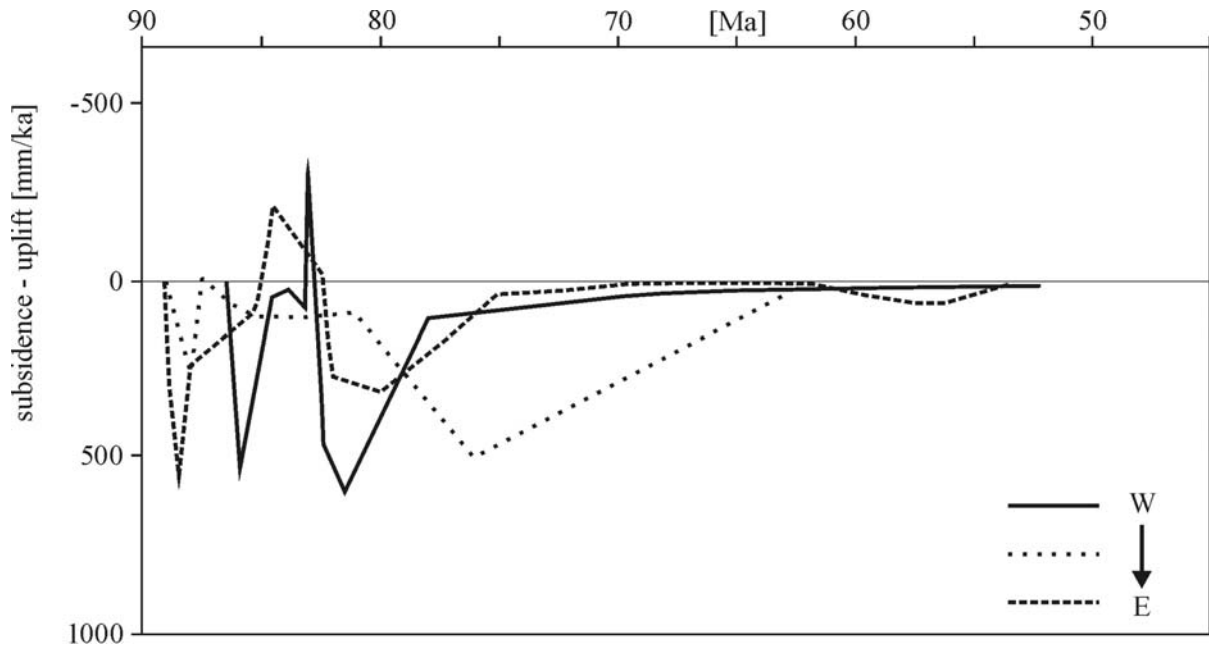


Figure 6.13: Subsidence and uplift curves for different localities (from W to E) of the Gosau group depocenters. Redrawn after Wagreich 1995. Sedimentation of the Gosau group terminated at around 50 Ma.

There is a striking similarity between our Rb/Sr deformation ages for the abandonment of the South Penninic paleosubduction interface, and the timing of the end of subsidence and sedimentation within the Gosau group depocenters, both at around 50 Ma (Eocene). Therefore, it is likely that there is a causal relationship between the end of deformation along the South Penninic-Austroalpine suture zone, and termination of Gosau group sedimentation. According to Wagreich (1995) the termination of the Gosau group sedimentation is associated with the end of tectonic erosion and the transformation of the erosive margin again back into an accretive one. We suggest that tectonic underplating and accretion of the Middle Penninic micro-continent, roughly at 50 Ma (e.g. von Blanckenburg and Davies 1995), accounts for the locking of the South Penninic subduction zone and associated termination of tectonically erosive mass transfer mode. Such accretive underplating may have resulted in the termination of Gosau group sedimentation, due to an accretion-related pulse of uplift.

6.7.5. Isotopic dating – a hint for mass transfer mode

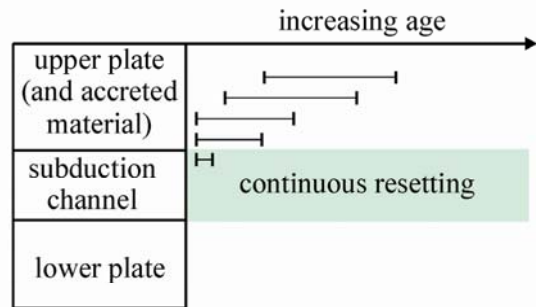
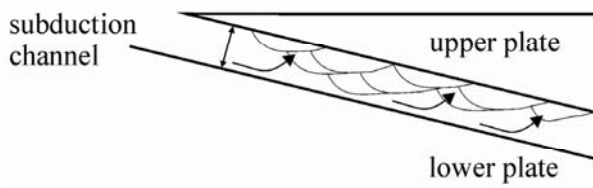
Our Rb/Sr isotopic age data provide another hint for the temporal evolution of mass transfer within the fossil subduction system. As illustrated in Figure 6.14 (a, b, c), hypothetical endmember scenarios for mass transfer mode within subduction channels comprise: 1) continuous underplating (addition of material to the base of the upper plate, i.e. basal accretion) (Fig. 6.14a), 2) continuous tectonic erosion removing material from the base of the upper plate (Fig. 6.14c), or 3) steady state, in a sense of continuous material flow neither adding nor removing material (Fig. 6.14b). For the isotopic record of deformation-sensitive isotopic systems in such endmember scenarios, the following predictions can be made:

Scenario a): A case scenario of continuous underplating (Fig. 6.14a) would result in a broad range of isotopic ages within the upper plate,

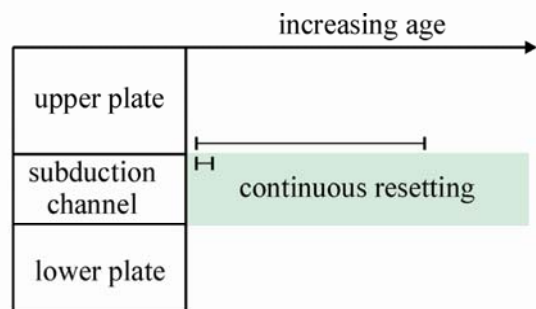
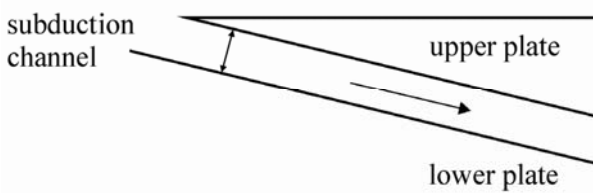
- getting systematically younger towards the subduction channel. Additionally, there would be a discrepancy between the ages obtained for the subduction mélange (comprising the subduction channel) and for the upper plate rocks at some distance from the channel. This would be caused by continuous accumulation of material at the base of the upper plate, and by associated transport of material out of the region of possible deformation-induced isotopic resetting.
- Scenario b): In the case of steady-state (continuous) material flow, isotopic ages for the upper plate would reflect the pre-subduction geological history, possibly with a domain of partial, subduction-related reset of age information at the base of the upper plate. A large non-systematic discrepancy between deformation ages from the subduction mélange (reflecting the latest stage of deformation), and the upper plate age record is expected (Fig. 6.14b). Continuous material flow within the subduction channel would constantly reset the isotopic systems, so that only the latest increment before abandonment would be preserved within the channel.
- Scenario c): Continuous tectonic erosion would result in nearly identical isotopic ages for both the basal parts of the upper plate and the subduction mélange due to ongoing mobilization of material at the base of the upper plate followed by tectonic removal to depth, which persistently shifts the region of deformation-induced isotopic resetting into the upper plate (Fig. 6.14c).
- Our Rb/Sr isotopic data are roughly identical for both the basal parts of the upper plate and the subduction mélange at

Figure 6.14: Hypothetical endmember scenarios for mass transfer mode within subduction channels. a) Continuous underplating adding material to the base of the upper plate (basal accretion). Assuming a snapshot in the evolution of such a system and analyzing the isotopic record, continuous underplating would result in a large spectrum of obtained isotopic ages within the upper plate, getting younger towards the subduction channel. Additionally, there would be a discrepancy between the ages obtained for the subduction mélange and the upper plate. b) Steady state continuous material flow neither adding nor removing material. Continuous material flow would result in a large spread of isotopic ages for the upper plate depending on its previous geological history. Additionally, a large discrepancy to the isotopic ages from the subduction mélange would be observable. c) continuous tectonic erosion removing material from the base of the upper plate. Continuous tectonic erosion would result in nearly identical isotopic ages for both the basal parts of the upper plate and the subduction mélange. d) Proposed temporal evolution path for material comprising the plate interface zone (red path): At first, tectonic erosion at the base of the upper plate removed constantly material. Thereby, the region of deformation induced resetting is shifted further into the upper plate, resulting in an identical isotopic record. At a certain time, the material may be located completely within the area of isotopic resetting. Abandonment of the subduction channel is caused by the basal accretion of the Middle Penninic micro-continent. Thereby, material from both the upper plate and the subduction mélange of the terminated South Penninic subduction zone are shifted out of the area of deformational resetting. This allows the preservation of the isotopical and deformational. Alternatively, material may have continuously entered and left the area of isotopic resetting by spatiotemporal changes of tectonic erosion and accretion, until it finally got resetted, accreted and removed out of the actively deforming system (blue path).

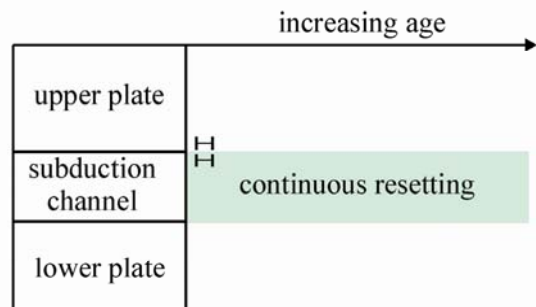
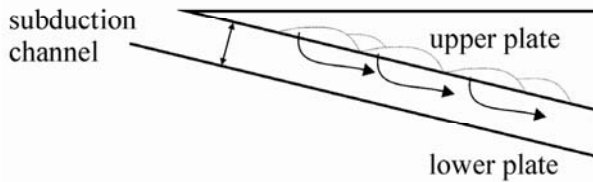
a continuous underplating (basal accretion)



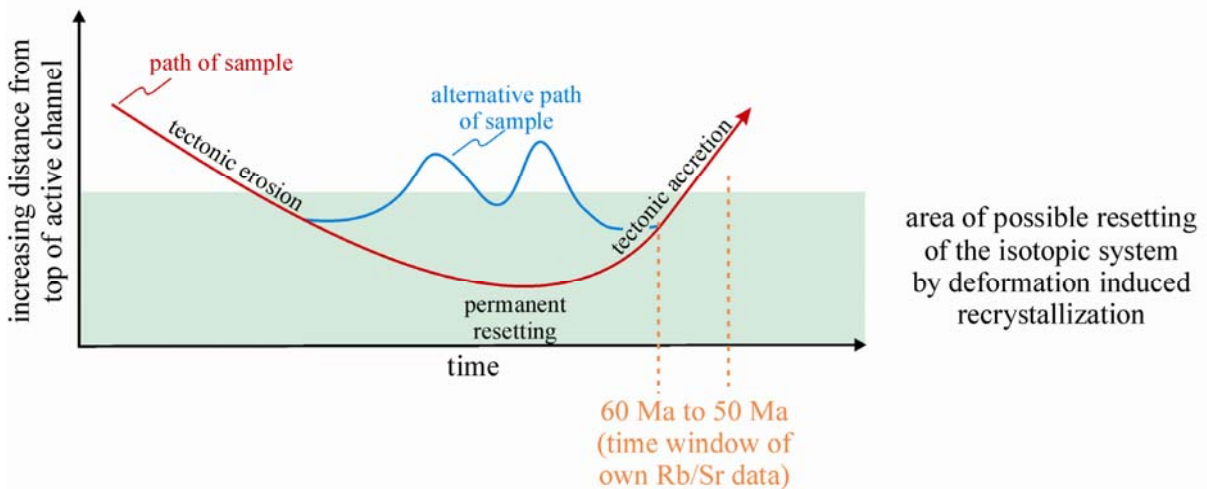
b continuous material flow



c continuous tectonic erosion



d model of suggested temporal evolution



around 50 Ma (Fig. 6.11b). Referring to the endmember scenarios above, this favors tectonic erosion as the main material transfer mode active within the subduction channel until the time of abandonment of this major suture zone. This is also in line with the observed numerous upper plate clasts embedded within the subduction mélange (e.g. Oncken 1998, Chapter 4) and the postulation by e.g. Wagneich (1991, 1995) that tectonic erosion is required for the formation of the Gosau group basins contemporaneously to the activity of the South Penninic subduction zone. Abandonment of the South Penninic-Austroalpine plate interface zone is most likely caused by the underplating of the Middle Penninic micro-continent (see Chapter 6.8.3.), leading to a transfer of the zone of active deformation further into the footwall. Thenceforward, the South Penninic-Austroalpine suture zone formed part of the upper plate, now passively overriding the Middle Penninic domain. This resulted in the preservation of the isotopic record of the final increment of subduction-related mass transfer along the South Penninic-Austroalpine plate interface zone.

Therefore, we propose the following temporal evolution path for material comprising the plate interface zone (red path in Fig. 6.14d): At first, tectonic erosion at the base of the upper plate constantly removed material from here. Thereby, the region of deformation-induced resetting is shifted further into the upper plate, resulting in an identical isotopic record for both the upper plate base and the subduction mélange. At a certain time, the material may be located completely within the area of isotopic resetting. Abandonment of the subduction channel is caused by the basal accretion the South Penninic subduction mélange. Thereby, material from both the upper plate and the subduction mélange of the terminated South Penninic subduction zone

is shifted out of the area of deformational resetting. Further on, the accretion of the Middle Penninic domain to the base of the South Penninic subduction mélange supports this process. This allows the preservation of the isotopic and deformational record for the final increment of subduction of the South Penninic ocean underneath the Austroalpine upper plate. Since the here proposed material path is simplified, alternatively, material may have continuously entered and left the area of isotopic resetting by spatiotemporal changes of tectonic erosion and accretion, until it finally got resetted, accreted and removed out of the actively deforming system (blue path in Fig. 6.14d). The slightly older Rb/Sr ages obtained for unstable slip in the basal part of the Austroalpine upper plate (pseudotachylyte ages ~75 Ma, Thöni 1988), and our own pseudotachylyte Ar/Ar data (60 Ma to 80 Ma, see Chapter 5) support this assumption (Fig. 6.11b). Ages obtained in the footwall of the abandoned South Penninic-Austroalpine suture zone for the Middle Penninic domain point to deformation at around 38 Ma (Ar/Ar synkinematic white mica ages, Markley 1995) (Fig. 6.11b). This is slightly younger than the ages obtained for the South Penninic-Austroalpine plate interface zone, which later on formed the hanging wall passively overriding the Middle Penninic domain. This would argue, at least partly, for continuous material flow along the newly developed deformation zone in the footwall of the South Penninic mélange subsequent to the termination of the South Penninic subduction zone resulting in an age gap between the hanging wall and footwall (Figs. 6.11b, 6.14). This provides an additional hint for spatiotemporal changes of material transfer mode and thereby caused changes of the position of the area of possible isotopic resetting (Fig. 6.14d).

Therefore, precise studies of the isotopic record of fossil subduction complexes have the potential to constrain the long term evolution of mass transfer in terms of tectonic erosion, basal accretion and steady state material flow.

6.8. Conclusion

In this study we show first precise Rb/Sr age data for the termination of subduction-related deformation along the South Penninic-Austroalpine suture zone in the Eastern Swiss Alps. Rb/Sr multimineral data for strongly foliated rocks of both the South Penninic subduction *mélange* and the immediate hanging wall (Austroalpine) resulted in two age groups. The first group reflects pre-Alpine (Paleozoic to Jurassic) deformation events in the upper plate Austroalpine basement, the age information being disturbed by subsequent (Alpine?) overprint to apparently southward increasing degrees. The second group resulted in ages consistently around 50 Ma both in the *mélange* and the overlying Austroalpine, interpreted to reflect recrystallization in both units in response to late increments of deformation along the paleosubduction interface. A ~50 Ma metamorphic mobilisate points to syn-subductional dehydration, fluid activity and mineral precipitation. The dated waning of deformation along the paleosubduction interface is inferred to be due to final basal accretion of the former subduction channel material to the upper plate. According to our structural data, the latest increment of deformation at ~50 Ma is characterized by a roughly top-W direction of tectonic transport. Referring to published paleogeographic reconstructions, the end of subduction related deformation is best explained by the locking of the South Penninic paleosubduction interface due to underplating of the Middle Penninic micro-continent, a process that caused a relocation of convergence-related strain from the paleosubduction *mélange* into the

new, Middle Penninic footwall. The shutoff of sedimentation in the forearc Gosau basins is contemporaneous with basal accretion of the South Penninic *mélange* and the Middle Penninic units, both processes occurring in the Lower Eocene (~50 Ma). We hypothesize a causal link between the two events, with the change from tectonic erosion to basal accretion being responsible for a regional pulse of uplift, leading to inversion of the forearc basins.

Sr isotope signatures of marine (meta-) carbonates are shown to be governed by both the depositional and by the syn-subduction recrystallization histories. Strontium isotope stratigraphy for an undeformed reference sample from the Middle Penninic points to Upper Jurassic carbonate deposition onto this unit. In contrast, metamorphosed carbonate samples from the subduction *mélange* exhibit clear evidence for syn-metamorphic alteration by fluids. Elevated $^{87}\text{Sr}/^{86}\text{Sr}$ ratios of the metacarbonates indicate that the dominant source of syn-subduction fluids has been the devolatilization of old continental crustal material, probably of subducted continental detritus.

We propose that the mass transfer mode of a paleosubduction system can be constrained using the deformation age record of both the upper plate and the subduction channel *mélange*. In our case, combined evidence from identical Rb/Sr ages for the Austroalpine upper plate and the South Penninic subduction *mélange*, from the presence of upper plate clasts in the subduction *mélange*, and from the syn-subduction evolution of Gosau forearc basins, points to tectonic erosion as prevailing mass transfer mode during the time of subduction.

